

**BEARING CAPACITY OF RECTANGULAR FOOTING RESTING OVER
GEOGRID REINFORCED SAND UNDER ECCENTRIC LOADING**

**A THESIS SUBMITTED
IN PARTIAL FULFILLMENT OF THE REQUIREMENT
FOR THE AWARD OF THE DEGREE
OF
MASTER OF TECHNOLOGY
IN
CIVIL ENGINEERING**



SHAMSHAD ALAM

DEPARTMENT OF CIVIL ENGINEERING

NATIONAL INSTITUTE OF TECHNOLOGY, ROURKELA

ODISHA-769008

MAY-2014

**BEARING CAPACITY OF RECTANGULAR FOOTING RESTING OVER
GEOGRID REINFORCED SAND UNDER ECCENTRIC LOADING**

**A Thesis Submitted in Partial Fulfillment of the Requirement
for the Award of the Degree of
Master of Technology**

in

Civil Engineering

Under the Guidance and Supervision of

DR. C. R. PATRA

Submitted by

SHAMSHAD ALAM

(212CE1020)



DEPARTMENT OF CIVIL ENGINEERING

NATIONAL INSTITUTE OF TECHNOLOGY, ROURKELA

ODISHA-769008

MAY-2014



National Institute of Technology
Rourkela

CERTIFICATE

This is to certify that the project entitled "***Bearing Capacity of rectangular footing resting over geogrid reinforced sand under eccentric loading***" is a record of bonafide work and sincere efforts carried out by Shamshad Alam under my supervision and is submitted in partial fulfillment of the requirement for the award of the degree in Master of Technology in Civil Engineering with specialization in Geotechnical Engineering in the Department of Civil Engineering, National Institute of Technology, Rourkela, Odisha New Delhi.

It is further certified that the work presented in this project has not been submitted elsewhere for the award of the any degree or diploma.

Place: Rourkela

Date:

Dr. Chittaranjan Patra

Professor

Department of Civil Engineering

NIT Rourkela

Odisha - 769008

ACKNOWLEDGEMENTS

Above all else, I would like to express my earnest appreciation to my supervised **Prof. Chittaranjan Patra**, for his direction and consistent support and backing throughout the course of my work in the last one year. I genuinely acknowledge and esteem his regarded direction and support from the earliest starting point to the end of the project work.

I would like to thank **Prof. N. Roy, HOD, Civil Engineering Department**, National Institute of Technology, Rourkela, who have illuminated me throughout my research work.

I am additionally appreciative to **Prof. S.K. Das, Prof. S.P. Singh** and all other faculty members of Civil Engineering Department, NIT Rourkel for their valuable support during the my research work.

An exceptional expressions of gratitude to **Miss. Roma Sahoo**, Ph.D. Scholar of Civil Engineering Department, NIT Rourkela for her suggestions, remarks and whole backing all around the research work.

I am also appreciative to Mr. A. K Nanda, Technical Assistant, Geotechnical Engineering Laboratory, NIT Rourkela for his remarkable support during my research work.

I am also appreciative to Mr. Chamuru Suniani (Geotechnical Lab Attendant), Mr. Harihar Garnayak (Highway Lab Attendant) and Mr. Suraj for their support & co-operation throughout the project work.

At long last, I might want to thank my parents and family members especially to my brother **Dr. Naushad Alam** for their immovable backing and constant wellspring of inspiration.

Shamshad Alam

ABSTRACT

A number of works have been carried out for the evaluation of a ultimate bearing capacity of shallow foundation, supported by geogrid reinforced sand and subjected to centric load. Few experimental studies have been made on the calculation of bearing capacity of shallow foundation on geogrid-reinforced sand under eccentric loading. However these studies are for strip footings. The purpose of this research work is to conduct model tests in the laboratory by utilizing rectangular surface foundation resting over the reinforced sand. The model tests have been conducted using rectangular footing with $B/L=0.5$ & 0.33 . The average relative density kept up throughout all the tests is 69%. The sand is reinforced by multiple layers (2, 3 & 4) of geogrid. The eccentricity varies from 0 to $0.15B$ with an increment of $0.05B$. Distance of first layer of geogrid layer from bottom of footing and the distance between two consecutive geogrid layers have been kept constant. The load settlement curve for each tests have been plotted to calculate ultimate bearing capacity. Parametric studies have been made to find the impact of eccentricity on bearing capacity of the foundation. The ultimate bearing capacity of eccentrically loaded square footings can be computed by knowing the ultimate bearing capacity of square footing under central load and a reduction factor (R_{kR}) for reinforced condition. The reduction factor is developed based on the results of laboratory model tests on geogrid reinforced soil. The ultimate bearing capacity of eccentrically loaded rectangular footing resting over geogrid reinforced sand can be calculated by knowing the ultimate bearing capacity of rectangular footing resting over reinforced sand bed and subjected to central vertical load by using reduction factor (R_{kR}). An equation for reduction factor for rectangular footing resting over geogrid reinforced sand is developed based on laboratory model test results.

Keyword: Ultimate Bearing Capacity, Reinforced Sand Bed, Eccentric Loading

CONTENTS

Certificate	i
Acknowledgements	ii
Abstract	iii
Contents	iv
List of figures	vii
List of tables	ix

CHAPTER 1 INTRODUCTION

1.1 General	1
1.2 Scope of the present study	2
1.3 Objective of present study	3

CHAPTER 2 LITERATURE REVIEW

2.1 General	4
2.2 Footing resting on unreinforced soil	4
2.3 Footing resting over reinforced soil	12

CHAPTER 3 EQUIPMENTS AND MATERIALS

3.1 General	19
3.2 Material Used	19
3.2.1 Sand	19

3.2.2	Geogrid	21
3.3	Test Tank	22
3.4	Equipment Used	23
3.4.1	Static Loading Unit	23
3.4.2	Proving Ring	24
3.4.3	Dial Gauge	24
3.4.4	Model Footing	24

CHAPTER 4 MODEL TEST AND METHODOLOGY

4.1	General	25
4.2	Sample Preparation	25
4.2.1	Placement of Sand	25
4.2.2	Placement of Geogrid	26
4.3	Equipment Setup	27
4.4	Model Test Procedure	28
4.5	Model Test Series	29

CHAPTER 5 RESULTS AND ANALYSIS

5.1	General	30
5.2	Bearing Capacity of Unreinforced Sand	30
5.2.1	Model Test Result	30
5.3	Bearing Capacity of Geogrid Reinforced Sand	37
5.3.1	Model Test Result	37
5.4	Analysis of Test Result	47

5.4.1	Analysis of Rectangular Footing with $B/L=0.5$	47
5.4.2	Analysis of Rectangular Footing with $B/L=0.33$	51
CHAPTER 6	SUMMARIZED RESULTS CSOPE FOR FUTURE WORK	56
References		57

LIST OF FIGURES

3.1	Grain Size Distribution	20
3.2	Flexible Geogrid	21
3.3	Static Loading Unit	23
4.1	Cross section showing sand bed with multiple number of reinforcement	26
4.2	Placement of Geogrid During Experiment	27
4.3	Equipment Setup	28
5.1	Load Settlement Curve of Unreinforced Sand ($B/L=0.5$)	31
5.2	Load Settlement Curve of Unreinforced Sand ($B/L=0.33$)	31
5.3	Variation of q_u with e/B ($B/L=0.5$)	32
5.4	Variation of q_u with e/B ($B/L=0.33$)	33
5.5	Change in N_γ with ϕ for different size of footing (DeBeer, 1965)	34
5.6	Load Settlement Curve of Unreinforced Sand for $e/B=0.00$ and different B/L ratio	35
5.7	Load Settlement Curve of Unreinforced Sand for $e/B=0.00$ and different B/L ratio	35
5.8	Load Settlement Curve of Unreinforced Sand for $e/B=0.00$ and different B/L ratio	36
5.9	Load Settlement Curve of Unreinforced Sand for $e/B=0.00$ and different B/L ratio	36
5.10	Load Settlement Curve for $B/L=0.5$ & $N=2$ and different e/B	37
5.11	Load Settlement Curve for $B/L=0.5$ & $N=3$ and different e/B	38
5.12	Load Settlement Curve for $B/L=0.5$ & $N=4$ and different e/B	38
5.13	Load Settlement Curve for $B/L=0.33$ & $N=2$ and different e/B	39
5.14	Load Settlement Curve for $B/L=0.33$ & $N=3$ and different e/B	39

5.15	Load Settlement Curve for $B/L=0.33$ & $N=4$ and different e/B	40
5.16	Load Settlement Curve for $B/L=0.5$ & $e/B=0.00$ with different N	40
5.17	Load Settlement Curve for $B/L=0.5$ & $e/B=0.05$ with different N	41
5.18	Load Settlement Curve for $B/L=0.5$ & $e/B=0.10$ with different N	41
5.19	Load Settlement Curve for $B/L=0.5$ & $e/B=0.15$ with different N	42
5.20	Load Settlement Curve for $B/L=0.33$ & $e/B=0.00$ with different N	42
5.21	Load Settlement Curve for $B/L=0.33$ & $e/B=0.05$ with different N	43
5.22	Load Settlement Curve for $B/L=0.33$ & $e/B=0.10$ with different N	43
5.23	Load Settlement Curve for $B/L=0.33$ & $e/B=0.15$ with different N	44
5.24	Variation of $q_{UR(e)}$ with e/B for $B/L=0.5$	48
5.25	Variation of R_{KR} with d_f/B for $B/L=0.5$	49
5.26	Variation of R_{KR} with e/B for $B/L=0.5$	49
5.27	Variation of α_1 with e/B for $B/L=0.5$	50
5.28	Variation of $q_{UR(e)}$ with e/B for $B/L=0.33$	52
5.29	Variation of R_{KR} with d_f/B for $B/L=0.33$	52
5.30	Variation of R_{KR} with e/B for $B/L=0.33$	53
5.31	Variation of α_1 with e/B for $B/L=0.33$	54

LIST OF TABLES

2.1	Bearing Capacity Factor	7
2.2	Shape, Depth & Inclination Factor	8
3.1	Geotechnical Property of Sand	20
3.2	Property of Geogrid	22
4.1	The Sequence of Model Test Series	29
5.1	Theoretical Bearing Capacity of Unreinforced Sand Bed for $B/L=0.5$	32
5.2	Theoretical Bearing Capacity of Unreinforced Sand Bed for $B/L=0.33$	33
5.3	Bearing Capacity of Reinforced Sand Bed for $e/B=0.00$	45
5.4	Bearing Capacity of Reinforced Sand Bed for $e/B=0.05$	46
5.5	Bearing Capacity of Reinforced Sand Bed for $e/B=0.10$	46
5.6	Bearing Capacity of Reinforced Sand Bed for $e/B=0.15$	46
5.7	Experimental Reduction Factor for Eccentrically Loaded Footing Resting on Reinforced Sand Bed with $B/L=0.5$	47
5.7	Experimental Reduction Factor for Eccentrically Loaded Footing Resting on Reinforced Sand Bed with $B/L=0.33$	51
5.7	Comparison of Predicted Ultimate Bearing Capacity with those Observed from Experiment	55

INTRODUCTION

1.1 GENERAL

Foundation is the lower most hidden but very important part of any structure whether it is onshore or offshore structure. It is the part which receive huge amount of load from superstructure and distribute it to ground. So the foundation should be strong enough to sustain the load of superstructure. The performance of a structure mostly depends on the performance of foundation. Since it is a very important part, so it should be designed properly.

Design of foundation consists of two different parts: one is the ultimate bearing capacity of soil below foundation and second is the acceptable settlement that a footing can undergo without any adverse effect on superstructure. Ultimate bearing capacity means the load that the soil under the foundation can sustain before shear failure; while, settlement consideration involves estimation of the settlement caused by load from superstructure which should not exceed the limiting value for the stability and function of the superstructure.

Ultimate bearing capacity problem can be solved with the help of either analytical solution or experimental study. First one can be studied using theory of plasticity or finite element method, while the second is reached through performing laboratory model test.

A literature survey on this subject shows that the majority of the bearing capacity theories involve centric vertical load on the rectangular footing. However in some of the cases, footing undergo eccentric loading due to the eccentrically located column on footing or due to the horizontal force along with vertical load acting on the structure. Footing located at property line,

machine foundation, portal frame buildings are some examples where the foundations experience eccentric loading.

A foundation under load will undergo settlement due to the horizontal and vertical movement of soil particle below foundation. In case of centric vertical load on the footing, stress distribution will be uniform below the footing and the footing will undergo equal settlement at both edges. On the other hand if the load is eccentric, the stress distribution below the footing will be nonuniform causing unequal settlement at two edges which will result in the tilt of footing. The tilt will increase with the increasing eccentricity to width ratio (e/B). When eccentricity to width ratio (e/B) is greater than $1/6$, the edge of the footing away from load will lose its contact with the soil which will result in the reduction of effective width of footing and hence reduction of ultimate bearing capacity of foundation. Researchers are introducing reinforcing material like metal strip, geofome, geotextile and geogrid to enhance the ultimate bearing capacity of foundation. Now a days use of geogrid has increased due to its high tensile strength at low strain, open grid structure which causes bonding between geogrid and foundation soil, long service life, light weight. High modulus polymer materials like polypropylene and polyethylene are used to manufacture the geogrid. Geogrid may be of two type i.e. biaxial and uniaxial geogrid depending upon the nature of manufacturing.

1.2 OBJECTIVE OF PRESENT STUDY

The objective of the present study is

- a) To conduct load tests on model rectangular footings resting over reinforced sand bed subjected to vertical eccentric load.
- b) Different layers of geogrids are used as reinforcement
- c) To develop the empirical correlation for bearing capacity of eccentrically loaded footings on reinforced sand by knowing the bearing capacity of footing under centric load.

LITERATURE REVIEW

2.1 GENERAL

After going through the literature, it has been found that several researchers worked on foundation problem. Some researchers worked on unreinforced sand bed while some worked on reinforce sand bed. At the same time, some researchers based their study on the results of prototype laboratory model testing while some researchers used theories based on finite element and numerical analysis to develop formulas to predict ultimate bearing capacity. Results that are available is related to the enhancement of load bearing capacity of shallow foundation supported by sand reinforced with metal strip, metal bar, rope fibers, geotextile and geogrid. Some of these tests were conducted using model square foundation while others using model strip foundation. In this chapter, brief reviews of some literature are presented.

2.2 FOOTING RESTING ON UNREINFORCED SOIL

Terzaghi (1943) was first to proposed a theory to calculate the ultimate bearing capacity of shallow foundation. The foundation having depth less than or equal to width is considered as shallow foundation as per this theory. This theory assumed the foundation as strip foundation with rough base. The soil above the bottom of foundation is considered as the surcharge $q = \gamma D_f$. The failure zone under the foundation is distinguish into three part i.e. one triangular zone just below the foundation, two radial shear zone and two Rankine passive zone. Using the equilibrium analysis, Tarzaghi expressed the ultimate bearing capacity in the form of

$$q_u = c' N_c + q N_q + \frac{1}{2} \gamma B N_\gamma \quad (\text{Continuous and strip foundation})$$

$$q_u = 1.3c'N_c + qN_q + 0.4\gamma BN_\gamma \text{ (Square foundation)}$$

$$q_u = 1.3c'N_c + qN_q + 0.3\gamma BN_\gamma \text{ (Circular foundation)}$$

Where, c' = cohesion of soil, γ = unit weight of soil and $q = \gamma D_f$

N_c , N_q , N_γ is the bearing capacity factor and is given as

$$N_c = \cot \phi' \left[\frac{e^{2\left(\frac{3\Pi}{4} - \frac{\phi'}{2}\right) \tan \phi'}}{2 \cos^2 \left(\frac{\Pi}{4} + \frac{\phi'}{2}\right)} - 1 \right]$$

$$N_q = \left[\frac{e^{2\left(\frac{3\Pi}{4} - \frac{\phi'}{2}\right) \tan \phi'}}{2 \cos^2 \left(45 + \frac{\phi'}{2}\right)} \right]$$

$$N_\gamma = \frac{1}{2} \left(\frac{K_{p\gamma}}{\cos^2 \phi'} - 1 \right) \tan \phi'$$

Where $K_{p\gamma}$ = passive pressure coefficient

Meyerhof (1953) extended the bearing capacity theory of foundation under the central vertical load to eccentric and inclined load and gave a theory which is referred as effective area method. Analysis result of eccentric vertical loads on horizontal foundation is correlated with the result of model footing test on clay and sand. Further the theory is extended to central inclined loads on horizontal and inclined foundation and compared with model test result of footing on clay and sand. Finally both results are combined for the analysis of foundation with eccentric inclined load.

Meyerhof (1963) proposed a generalized equation for ultimate bearing capacity of any shape of foundation (strip, rectangular or square) since Terzaghi (1943) do not report the case of rectangular footing and also do not consider the shearing resistance across the failure surface in soil above the bottom of foundation. The equation for ultimate bearing capacity is as follow.

$$q_u = c' N_c F_{cs} F_{cd} F_{ci} + q N_q F_{qs} F_{qd} F_{qi} + \frac{1}{2} \gamma B N_\gamma F_{\gamma s} F_{\gamma d} F_{\gamma i}$$

Where $F_{cs}, F_{qs}, F_{\gamma s}$ = shape factor,

$F_{cd}, F_{qd}, F_{\gamma d}$ = depth factor and

$F_{ci}, F_{qi}, F_{\gamma i}$ = inclination factor,

Prakash and Saran (1971) put forward a relationship to calculate the ultimate load per unit length of strip foundation loaded with vertical eccentric load which is given as

$$Q_{ult} = B \left[c' N_{c(e)} + q N_{q(e)} + \frac{1}{2} \gamma B N_{\gamma(e)} \right]$$

Where, $N_{c(e)}, N_{q(e)}$ and $N_{\gamma(e)}$ is the bearing capacity factor in case of eccentric loading.

Vesic (1973) in his research, considered the effect of shape of footing, effect of shearing resistant of soil above the bottom of footing and proposed a relationship for shape factor. A number of researchers proposed different relationship for bearing capacity factor as well as shape and depth factor which is summarized below.

Table 2.1: Bearing Capacity Factor

Bearing Capacity Factor	Equation	Researchers
N_q	$N_q = \left[\frac{e^{2\left(\frac{3\Pi}{4} - \frac{\phi'}{2}\right)\tan\phi'}}{2\cos^2\left(45 + \frac{\phi'}{2}\right)} \right]$	Terzaghi (1943)
N_q	$N_q = e^{\Pi \tan\phi} \left(\frac{1 + \sin\phi}{1 - \sin\phi} \right)$	Prandtl (1921), Reissner (1924), Meyerhof (1951)
N_q	$N_q = \frac{40 + 5\phi}{40 - \phi}$	Krizek (1965)
N_c	$N_c = (N_q - 1)\cot\phi$	Prandtl (1921), Reissner (1924), Terzaghi (1943), Meyerhof (1951)
N_c	$N_c = \frac{228 + 4.3\phi}{40 - \phi}$	Krizek (1965)
N_γ	$N_\gamma = 1.8(N_q - 1)\cot\phi(\tan\phi)^2$	Terzaghi (1943)
N_γ	$N_\gamma = 1.5(N_q - 1)\tan\phi$	Lundgren and Mortensen (1953) and Hansen (1970)
N_γ	$N_\gamma = 2(N_q + 1)\tan\phi$	Caquot and Kerisel (1953), Vesic (1973)
N_γ	$N_\gamma = 1.8(N_q - 1)\tan\phi$	Biarez et al (1961)
N_γ	$N_\gamma = (N_q - 1)\tan(1.4\phi)$	Meyerhof (1963)
N_γ	$N_\gamma = \frac{6\phi}{40 - \phi}$	Krizek (1965)
N_γ	$N_\gamma = 1.5N_c \tan\phi^2$	Hansen (1970)

Table 2.2: Shape, Depth & Inclination Factor

Factors	Equation	Reference
Shape Factor	<p>For $\phi = 10^\circ$, $\lambda_{cs} = 1 + 0.2 \left(\frac{B}{L} \right)$</p> <p>$\lambda_{qs} = \lambda_{\gamma s} = 1$</p> <p>For $\phi \geq 10^\circ$ $\lambda_{cs} = 1 + 0.2 \left(\frac{B}{L} \right) \tan^2 \left(45 + \frac{\phi}{2} \right)$</p> <p>$\lambda_{qs} = \lambda_{\gamma s} = 1 + 0.1 \left(\frac{B}{L} \right) \tan^2 \left(45 + \frac{\phi}{2} \right)$</p>	Meyerhof (1963)
	<p>$\lambda_{cs} = 1 + \left(\frac{N_q}{N_c} \right) \left(\frac{B}{L} \right)$</p> <p>$\lambda_{qs} = 1 + \left(\frac{B}{L} \right) \tan \phi$</p> <p>$\lambda_{\gamma s} = 1 - 0.4 \left(\frac{B}{L} \right)$</p>	DeBeer (1970)
	<p>$\lambda_{cs} = 1 + (1.8 \tan^2 \phi + 0.1) \left(\frac{B}{L} \right)^{0.5}$</p> <p>$\lambda_{qs} = 1 + 1.9 \tan^2 \phi \left(\frac{B}{L} \right)^{0.5}$</p> <p>$\lambda_{\gamma s} = 1 + (0.6 \tan^2 \phi - 0.25) \left(\frac{B}{L} \right)$ (for $\phi \leq 30^\circ$)</p> <p>$\lambda_{\gamma s} = 1 + (1.3 \tan^2 \phi - 0.5) \left(\frac{L}{B} \right)^{1.5} e^{-\left(\frac{L}{B} \right)}$ (for $\phi > 30^\circ$)</p>	Michalowski (1997)

Table 2.2: (Continued)

Factors	Equation	Reference
Depth factor	<p>For $\phi = 0$, $\lambda_{cd} = 1 + 0.2 \left(\frac{D_f}{B} \right)$</p> <p>$\lambda_{qd} = \lambda_{\gamma d} = 1$</p> <p>For $\phi \geq 10$ $\lambda_{cd} = 1 + 0.2 \left(\frac{D_f}{B} \right) \tan \left(45 + \frac{\phi}{2} \right)$</p> <p>$\lambda_{qd} = \lambda_{\gamma d} = 1 + 0.1 \left(\frac{D_f}{B} \right) \tan \left(45 + \frac{\phi}{2} \right)$</p>	Meyerhof (1963)
	<p>For $\frac{D_f}{B} \leq 1$ $\lambda_{cd} = 1 + 0.4 \left(\frac{D_f}{B} \right)$ (for $\phi = 0$)</p> <p>$\lambda_{cd} = \lambda_{qd} - \frac{1 - \lambda_{qd}}{N_q \tan \phi}$</p> <p>$\lambda_{qd} = 1 + 2 \tan \phi (1 - \sin \phi)^2 \left(\frac{D_f}{B} \right)$</p> <p>$\lambda_{\gamma d} = 1$</p> <p>For $\frac{D_f}{B} > 1$ $\lambda_{cd} = 1 + 0.4 \tan^{-1} \left(\frac{D_f}{B} \right)$</p> <p>$\lambda_{qd} = 1 + 2 \tan \phi (1 - \sin \phi)^2 \tan^{-1} \left(\frac{D_f}{B} \right)$</p> <p>$\lambda_{\gamma d} = 1$</p> <p>$\left[\text{Note : } -\tan^{-1} \left(\frac{D_f}{B} \right) \text{ is in Radians.} \right]$</p>	Hansen (1970)

Purkayastha and Char (1977) used method of slice to analyze the eccentrically loaded strip footing resting on sand layer. Based on their study, they proposed a relationship for reduction factor which is given as

$$R_k = a \left(\frac{e}{B} \right)^k$$

Where R_k = reduction factor

a and k is the function of D_f/B as tabulated below

D_f/B	a	k
0.00	1.862	0.73
0.25	1.811	0.785
0.50	1.754	0.80
1.00	1.820	0.888

Now the ultimate bearing capacity of eccentrically loaded strip footing is given by

$$q_{u(eccentric)} = q_{u(centric)} (1 - R_k)$$

$$q_{u(centric)} = q N_q F_{qd} + \frac{1}{2} \gamma B N_\gamma F_{\gamma d}$$

Highter and Anders (1985) made a theoretical approach to find out the effective area of rectangular footing subjected to a load eccentric in both direction. Four possible cases of eccentricity are considered by the author.

Case I:- $e_L / L \geq \frac{1}{6}$ and $e_B / B \geq \frac{1}{6}$. The active area is given by

$$A' = \frac{1}{2} B_1 L_1$$

$$\text{Where, } B_1 = B \left(1.5 - \frac{3e_B}{B} \right) \quad \& \quad L_1 = L \left(1.5 - \frac{3e_L}{L} \right)$$

Case II:- $e_L / L < 0.5$ and $0 < e_B / B < \frac{1}{6}$. The active area is given by

$$A' = \frac{1}{2} (L_1 + L_2) B$$

Where, L_1 & L_2 will be taken from graph given by Highter and Anders (1985).

Case III:- $e_L / L < \frac{1}{6}$ and $0 < e_B / B < 0.5$. The active area is given by

$$A' = \frac{1}{2} (B_1 + B_2) L$$

Where, B_1 & B_2 will be taken from graph given by Highter and Anders (1985).

Case IV:- $e_L / L < \frac{1}{6}$ and $e_B / B < \frac{1}{6}$. The active area is given by

$$A' = L_2 B + \frac{1}{2} (B + B_2) (L - L_2)$$

Where, B_2 & L_2 will be taken from graph given by Highter and Anders (1985).

2.3 FOOTING RESTING OVER REINFORCED SOIL

Huang and Tatsuoka (1990) performed a number of plane strain model test on a strip footing. The effect of length, the arrangements, the rigidity and the breaking strength of reinforcement were scrutinized systematically. The strain field in sand, the tensile force in reinforcement and the distribution of contact pressure on footing were measured. Based on the test result, a method of stability analysis by the limit equilibrium method was developed, taking into account the effect of the arrangement and properties of reinforcement and the failure mode of reinforced sand. The test result shows that the bearing capacity in sand can increase largely by reinforcing the zone immediately beneath the footing with stiff short reinforcement layer having only a length equal to the footing width.

Khing et. al. (1993) performed laboratory model test for bearing capacity of strip foundation supported by sand reinforced with a number of geogrid. Based on the model test result, BCR based on ultimate bearing capacity and at level of limited settlement of the foundation has been determined. The BCR calculated on the basis of limited settlement appears to be about 60-70% of the ultimate BCR.

Das and Omar (1994) performed laboratory model test to calculate the ultimate bearing capacity of surface strip foundation on geogrid reinforced sand and unreinforced sand. Effect of width of foundation and relative density of sand bed were also observed by changing these parameter. Model test result shows that BCR of given sand geogrid system decreases with increase in foundation width and reached to a practically constant value when width of foundation is equals or greater than about 130-140mm.

Das et. al. (1994) performed laboratory model test for ultimate bearing capacity of strip foundation supported by geogrid reinforced sand and saturated clay. On the basis of model test

result, the optimum depth and width of reinforcing layers and the optimum depth of location of the first layer of geogrid in sand and saturated clay were determined and compared. Test result shows that the settlement of strip foundation at ultimate load on reinforced and unreinforced clay is practically same while in case of sand, an increase in ultimate load brought about by the reinforcement is accompanied by an increase in the settlement of the foundation. For maximum BCR, the optimum width of geogrid layer is $8B$ for sand and $5B$ for clay.

Yetimoglu et. al. (1994) performed laboratory model test as well as finite element analysis to investigate the ultimate bearing capacity test of centrically loaded rectangular footing on geogrid reinforced sand. The test indicated that optimum embedment depth was approximately $0.3B$. The analysis indicated that the optimum depth would be somewhat larger for settlement ratios greater than 6%. For multilayer reinforced sand, the highest bearing capacity occurs at an embedment depth of approximately $0.25B$.

Zhao (1996) presented a failure criterion for a reinforced soil composite and described the slip line equation for reinforced soil. Also calculate the failure load and stress characteristics for reinforced slope, wall and foundation. The result shows that inclusion of reinforcement enlarges the plastic failure region in reinforced soil structure and significantly increases the load capacity.

Huang and Menq (1997) evaluate the bearing capacity characteristics of sandy ground reinforced with horizontal reinforcing layer by performing a total of 105 model test. The result of 105 model test is analyzed using calibrated internal friction angle of sand. This study is based on two failure mechanism i.e. deep-footing and wide-slab mechanism. The improvement in bearing capacity is because reinforcement below the footing act like a quasi-rigid, wide earth slab. An attempt is made to maximize the bearing capacity by optimizing the depth and width of quasi-

rigid earth slab. Based on their study, they proposed a relationship to determine the ultimate bearing capacity based on wide-slab mechanism.

$$q_{u(R)} = 0.5(B + \Delta B)\gamma N_\gamma + \gamma d N_q$$

$$\Delta B = 2d \tan \beta$$

Where, B = width of footing, N_q & N_γ = bearing capacity factor, γ = working density of sand
 d = depth of last reinforcement layer measured from the bottom of footing and is given by

$$d = u + (N - 1)h$$

Where, u = depth of first layer of reinforcement from the bottom of footing, N = number of reinforcement layer and h = spacing between two consecutive reinforcement layer.

$$\tan \beta = 0.68 - 2.071\left(\frac{h}{B}\right) + 0.743(CR) + 0.03\left(\frac{b}{B}\right)$$

Where, CR = cover ratio and is given by (w/W) where w = width of longitudinal ribs and W = center-to-center spacing of longitudinal rib, b = width of reinforcement layer.

Dash et. al. (2001) performed laboratory model test on strip footing supported by sand bed reinforced with geocell mattress. The test is performed by changing the pattern of geocell formation, pocket size, height and width of geocell mattress, tensile stiffness of geogrid used to make the geocell and relative density of sand. The result shows that pressure-settlement behavior of strip footing resting on geocell reinforced sand is approximately linear even up to a settlement of about 50% of footing width and a load as high as 8 times the ultimate capacity of unreinforced one.

Shin et. al. (2002) performed small scale laboratory model test to determine the ultimate bearing capacity of strip foundation supported by geogrid reinforced sand. For the test, embedment ratio of the foundation was varied from zero to 0.6. The result shows that for a given reinforcement-depth ratio, u/B , h/B , and b/B the BCR_u increases with the embedment ratio of the foundation (D_f/B).

Kumar and Saran (2003) extend the method of analysis of strip footing on reinforced earth presented by Binquet and Lee (1975) and Kumar and Saran (2001) to rectangular footing on reinforced sand. The validation has been done with large scale model test conducted by Adams and Collin (1997). An empirical method has been proposed for determination of ultimate bearing capacity of reinforced soil.

Kumar et. al. (2005) proposed a method to obtain the pressure-settlement characteristics of rectangular footings resting on reinforced sand based on constitutive law of soil. The effect of weight of soil mass has been considered in determination of stress. The base of footing has been assumed smooth, as effect of roughness on pressure-settlement characteristics has been found to be negligible Saran (1977). Stresses in soil mass have been computed using theory of elasticity. Strains have been computed from the hyperbolic soil model defined by Kondner (1963). The analysis has been validated with the model test result conducted by Kumar (1997). Predicted and model test result match well up to two-third of ultimate bearing pressure.

Patra et. al. (2005) presented laboratory model test result of strip foundation supported by multi-layered geogrid-reinforced sand. Embedment depth of foundation is the variable (0 to $1B$) parameter in this study. The ultimate bearing capacity obtained from the model test result has been compared with the theory proposed by Hung and Menq (1977). The result of this study shows that the BCR increases with the increase in embedment ratio.

Omar (2006) conducted the laboratory model test for ultimate bearing capacity of eccentrically loaded strip foundation supported by multilayer geogrid reinforced sand. Based on the laboratory model test, an empirical relationship for reduction factor has been developed. This relationship can be used to calculate ultimate bearing capacity of eccentrically loaded strip footing if ultimate bearing capacity of centrally loaded strip footing is available. The reduction factor R_k is calculated as

$$R_k = 5.11 \left(\frac{D_f}{B} \right)^{-0.14} \left(\frac{e}{B} \right)^{1.21}$$

Patra et. al. (2006) presented a result of laboratory model test conducted to determine the ultimate bearing capacity of eccentrically loaded strip foundation supported by geogrid reinforced sand. The depth of foundation was only the variable and varied from zero to B. Based on the laboratory model test, an empirical relationship for reduction factor has been developed to calculate the ultimate bearing capacity of eccentrically loaded strip foundation. The reduction factor R_k is calculated as

$$R_k = 4.97 \left(\frac{d_f}{B} \right)^{-0.12} \left(\frac{e}{B} \right)^{1.21}$$

This reduction factor can be used in the bearing capacity formula given by Purkayastha and Char (1977) which is shown below.

$$\frac{q_{u(e)}}{q_{u(e=0)}} = 1 - R_k$$

Kumar et. al. (2007) investigated the ultimate bearing capacity of strip footing supported by reinforced and reinforced subsoil consisting of a strong sand layer overlying a low bearing

capacity sand deposit. Based on the model test result, the effect of stratified subsoil on foundation bearing capacity, the effect of reinforcing the top layer with horizontal layers of geogrid reinforcement on the bearing capacity and effect of reinforcing stratified subsoil on the settlement of the foundation has been analyzed. The result showed that there is up to 3 to 4 times increase in ultimate bearing capacity of strip footing resting on sand after replacing the top 1B thick layer of existing weak soil with well graded sand layer and reinforcing it with 2–4 layers of geogrid reinforcement.

Basudhar et. al. (2008) analyzed the behavior of a geotextile-reinforced sand-bed subjected to strip loading using the finite element method. The soil–geotextile interaction has been modeled by assigning the contact conditions at the interface. Based on the parametric study it has been found that for a single layer of geotextile

Latha and Somwanshi (2009) presented the laboratory model test and numerical simulation result for bearing capacity of square footing resting on geosynthetic reinforced sand. The effect of various reinforcement parameters like the type and tensile strength of geosynthetic material, number of reinforcement, layout and configuration of geosynthetic layer below the footing is studied. Model test result shows that effective depth of the zone of reinforcement below square footing is twice the width of footing, the optimum spacing of reinforcement layer is about 0.4 times the width of footing and the optimum width of reinforcement is 4 times the width of footing.

Sadoglu et. al. (2009) performed laboratory model test with eccentrically loaded strip footing on geotextile-reinforced dense sand to investigate the effect of eccentricity on ultimate bearing capacity of foundation. Experimental result is compared with commonly used approaches such as Meyerhof's (1953) effective width concept.

Nareeman (2012) performed experimental work with circular, square and rectangular footing to study the effect of scale on bearing capacity and settlement of footing. Then the experimental result is compared with finite element analysis result. Model test results show that the bearing capacity factor N_γ is dependent on the absolute width of the footing and N_γ for dense soil decreases with increasing of footing size.

Kolay et. al. (2013) investigated the ultimate bearing capacity of rectangular footing supported by geogrid reinforced silty clay soil with thin layer of sand on the top. Initially one geogrid is placed at the interface of soil with u/B equals to 0.667 and it is found that bearing capacity increases with an average of 16.67% and when one geogrid is placed at the middle of sand layer with u/B equals 0.33, bearing capacity increases with an average of 33.33%.

Kumar et. al. (2013) proposed an analytical procedure based on non-linear constitutive laws of soils to obtain pressure-settlement characteristics of strip footings resting on layered reinforced sand. The confining effect of the reinforcement provided in the soil at different layers has been incorporated in the analysis by considering the equivalent stresses generated due to friction at the soil-reinforcement interface. Result shows that predicted and model test result match well up to two-third of ultimate bearing pressure.

EQUIMENTS AND MATERIALS

3.1 GENERAL

The basic aim of this research is to discover the bearing capacity of reinforced sand bed. So the sand is the basic material which is used in this research work. Tensar Biaxial geogrid is used to reinforcing the sand. Hydraulic static loading machine is used to apply the concentrated load on the mild steel footing which is transferred to sand bed in form of distributed load. Test tank of dimension 1 X 0.504 X 0.655 m is used to prepare the sand bed.

3.2 MATERIAL USED

3.2.1 SAND

a) Sample Collection

The sand used in research work is collected from nearby Koel river. The sand is washed to make it free from soil, grass roots, and other organic materials and then the washed sample is dried in oven. The oven dried sample is first sieved on 710 μ IS sieve and then the sand passing through 710 μ IS sieve is again sieved on 300 μ IS sieve. The sand sample retained by 300 μ IS sieve is used for research work.

b) Characteristics of Sand

All experiments are conducted at same relative density of 69%. The average unit weight of sand at this relative density is 1.46g/cc and internal friction angle is found out to be 40.9⁰ by direct shear test at this relative density. The characteristics of sand used in research work and the grain size distribution is listed in table 3.1 and figure 3.1 respectively.

Table 3.1: Geotechnical Property of Sand

Property	Value
Specific gravity (G)	2.64
Effective particle size (D_{10})	0.33mm
Mean particle size (D_{50})	0.455mm
(D_{60})	0.47mm
(D_{30})	0.42mm
Coefficient of uniformity (C_u)	1.424
Coefficient of curvature (C_c)	1.137
Maximum unit weight	14.87 kN/m ³
Minimum unit weight	13.42kN/m ³
Angle of internal friction (ϕ degree)	40.9 ⁰
Maximum void ratio (e_{max})	0.929
Minimum void ratio (e_{min})	0.741

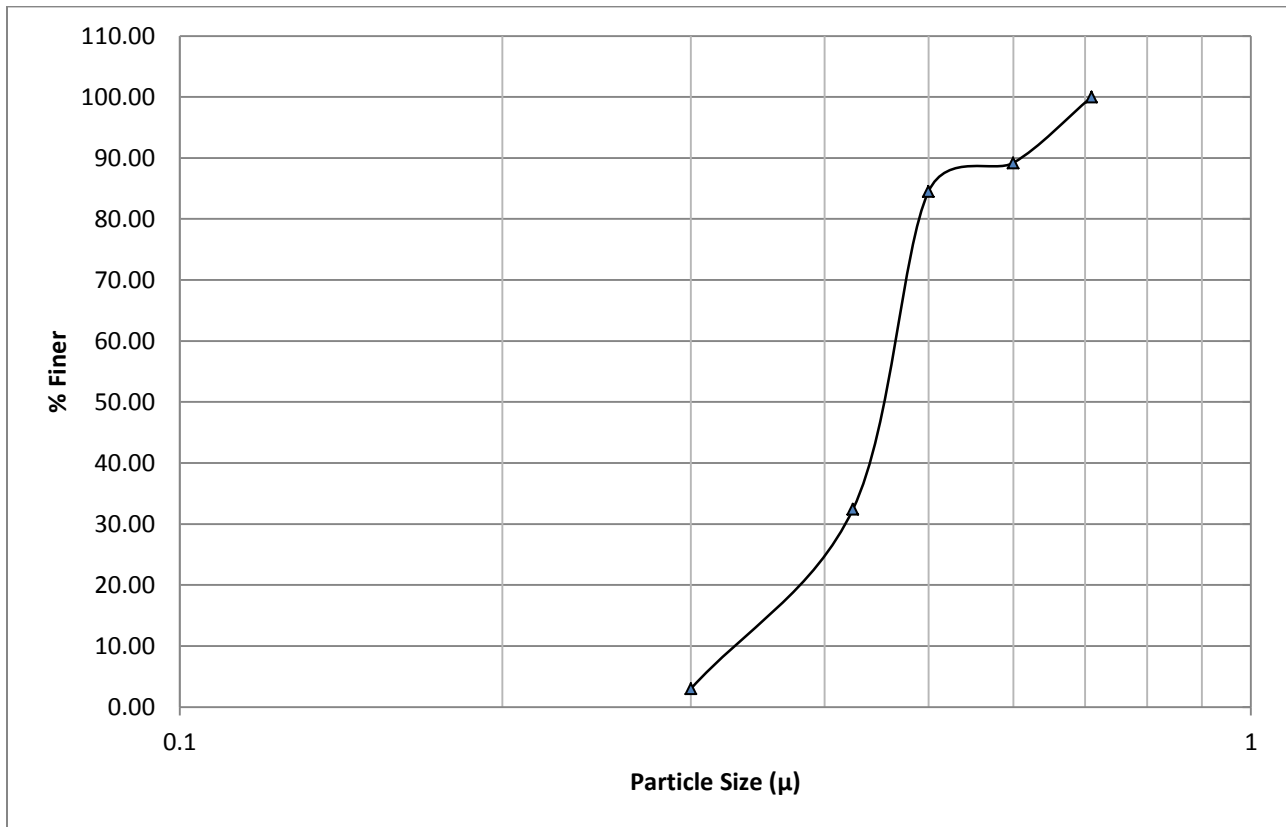


Figure 3.1. Grain Size Distribution

3.2.2 GEOGRID

Geogrids form a separate type of geosynthetics designed for reinforcement. Geogrids are categorized by a relatively high tensile strength and a uniformly distributed group of large openings in between longitudinal and transverse rib. These openings are called apertures. The openings allow sand particles on either side of the mounted geogrid to come in direct contact which increases the interaction between the geogrid and sand. The geogrid features vary in polymer type and cross-sectional proportions. Geogrids are manufactured using high modulus polymer materials like polypropylene and high density polyethylene and are either inherently manufactured, ultrasonically or glue bonded. On the basis of strength direction, geogrids are classified as Biaxial and Uniaxial while classified as Rigid and Flexible based on rigidity.

The flexible geogrids as shown in figure 3.1 are manufactured by high tenacity polyester or propylene yarns that are typically twisted together. The single yarns are then weaved or knitted forming flexible junctions.

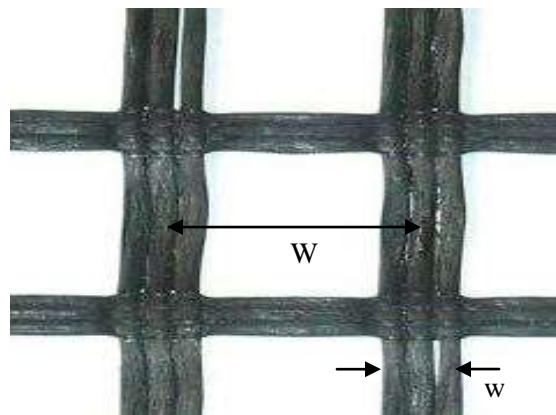


Figure 3.2. Flexible Geogrid

Geogrid used in present model test is biaxial flexible geogrid whose physical characteristics are shown in Table 3.2.

Table 3.2. Properties of the geogrid

Parameters	Value
Polymer	Polypropylene Pp
Tensile strength at 2% strain	7 KN/m
Tensile strength at 5% strain	14 KN/m
Aperture size (W)	39*39 mm
Aperture shape	Square
Rib width (w)	1.1 mm
Junction strength	95%

3.3 TEST TANK

Tank size is decided on the basis of IS code and from the result of some literature. IS 1888-1962 says that minimum size should be at least 5 times the width of test plate to develop the full failure zone without any interference of side. For cohesionless soil, Chumar (1972) suggested that the maximum extension of failure zone will be 2.5 times of the footing width along the side and 3 times the width of footing below the footing. Keeping the above criteria in mind, 1m long tank with 0.504m width and 0.655m height has been used for $10\text{cm} \times 20\text{cm}$ footing and 1.8m long tank with 0.504m width and 0.655m height has been used for $10\text{cm} \times 30\text{cm}$ footing during experimental work. Due to the tank size, there may be some scale effect which will influence the ultimate bearing capacity of footing resting over geogrid reinforced sand bed. Since tests under both the loading condition (i.e. centric and eccentric) have been conducted in same tank, there will not be any effect on the reduction factor (R_{KR}) since reduction factor is defined as $\left(1 - \frac{q_{uR(e)}}{q_{uR(e=0)}}\right)$. Where

$q_{uR(e)}$ and $q_{uR(e=0)}$ are the ultimate bearing capacity of reinforced sand bed under eccentric and centric loading respectively.

The tank is made up of 8mm thick mild steel plate with 12mm thick high strength fiber glass on two longitudinal side to make this side transparent. Horizontal bracings of 6mm thick flat are provided on the all four sides of tank to prevent bulging of side during experimental work. A number of scales are fitted on the inner face of tank wall to ensure the height of fall and density during the sample preparation.

3.4 EQUIPMENT USED

3.4.1 STATIC LOADING UNIT

A hydraulically operated static loading unit is used to apply the load on the foundation during test. The whole loading unit consist of one electrical panel, one power pack and one loading frame with shaft. Power pack consist of one oil tank filled with oil which is used to develop hydraulic pressure and it also consist of several valves to control the flow of oil to loading unit and hence control the movement of shaft. The shaft is supported by a horizontal beam which provide the reaction to the shaft during application of load.

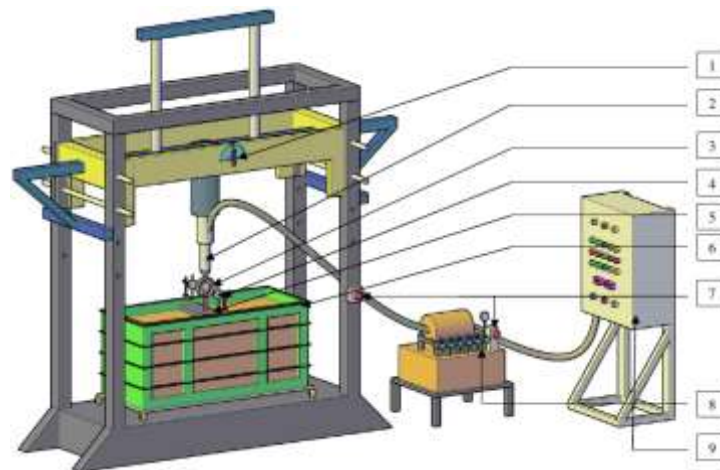


Figure 3.3 Static Loading Unit

Legend of Figure 3.3 (Static Loading Unit)

1. Inclination Indicator	4. Dial Gauge	7. Pressure Adjustable Knob
2. Hydraulic Cylinder	5. Model Footing	8. Hydraulic Power Pack
3. Proving Ring	6. Test Tank	9. Electrical Control Panel

3.4.2 PROVING RING

Proving ring of 20kN, 25kN, 50kN & 100kN is used during experiment to measure the applied load on the foundation during the experimental work. Top of proving ring is attached with the movable shaft of static loading unit while the bottom is in contact with the metallic ball which is resting on the footing. When load is applied, the load is transmitted from proving ring to the footing via this metallic ball.

3.4.3 DIAL GAUGE

Two number of dial gauge which can measure settlement up to 50mm with least count of 0.01mm is used during the experimental work. Needle of the dial gauge is placed on the two diagonally opposite corner of the footing. Magnetic base which is supported by test tank is used to support the dial gauge.

3.4.4 MODEL FOOTING

Model footing of thickness 3cm made up of mild steel is used for experimental work. A 1cm deep circular groove is made to hold the metallic ball on one face of the footing at center and at an eccentricity of 0.05B, 0.1B & 0.15B from the center on the separate footings. Sand is applied on the other face of footing with the help of epoxy glue to make it rough so that friction between footing and foundation soil can develop during application of load.

MODEL TEST AND METHODOLOGY

4.1 GENERAL

To study the bearing capacity of eccentrically loaded foundation, laboratory model test has been performed on rectangular footing resting on sand bed reinforced with multilayered geogrid. Model test is performed on sand remolded at one density, footing with eccentricity varied from 0 to $0.15B$ and number of reinforcement varied as 0, 2, 3 & 4. Footing is resting on the surface of reinforced sand bed i.e. depth of embedment is zero in the test. Metallic ball is used as load transferring medium between shaft and model footing.

4.2 SAMPLE PREPARATION

4.2.1 PLACEMENT OF SAND

Internal dimension of the test tank is measured and weight of sand to fill the tank upto a specified height is calculated using working density of 1.46gm/cc . Now sever trials are made to discover the height of fall of sand by allowing the sand to fall from different height to filling the tank up to desired height. After filling the tank upto desired height using raining technique, density of sand filled in tank for different trials is calculated. Height of fall for which the density is same as working density is taken for sample preparation. After finding out the height of fall, weight of sand require for 2.5cm thick layer to maintain the working density is taken and poured into the tank from specified height of fall using sand raining technique. Each layer is levelled using level plate to check whether the density is maintained properly or not. For the preparation of reinforced sand sample, geogrid is placed at desired depth from bottom of footing after levelling the surface to make it horizontal. Placement of geogrid is described in detail in section 4.2.2.

4.2.2 PLACEMENT OF GEOGRID

In case of reinforced sand bed, it is very essential to decide the magnitude of u/B and b/B to take the maximum advantage in bearing capacity of reinforced sand. After going through several literature, it has been found that $(u/B)_{cr}$ for strip foundations vary between 0.25 and 0.5, $(b/B)_{cr}$ is 8 and 4.5 for strip footing and square footing respectively and $(h/B)_{cr}$ lies between 0.25 to 0.4. By keeping the above factor in mind, for this test these factors are fixed as $(u/B) = 0.35$, $(b/B) = 4.5$ & $(h/B) = 0.25$.

Since in this test, width of footing B is 10cm so width of geogrid b is taken as 4.5cm. The depth of first layer u from bottom of footing is taken as 3.5cm and distance between each consecutive layer h is taken as 2.5cm. During the sample preparation, square shaped geogrid of size 4.5cm has been taken and placed below the footing with first layer at the depth of 3.5cm and other layers with 2.5cm distance between two consecutive geogrid layer as shown in Figure 4.1.

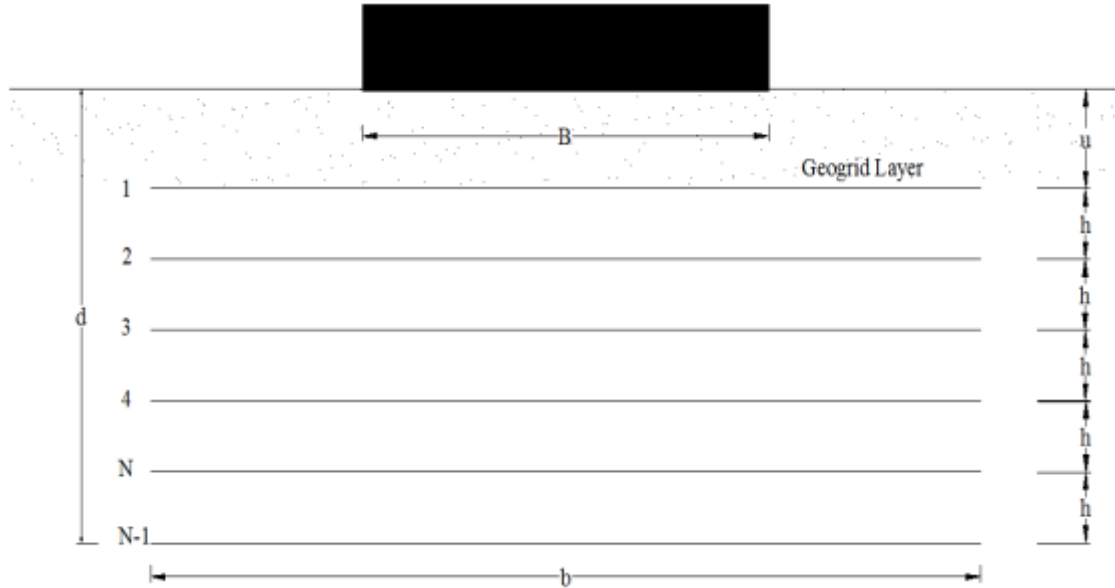


Figure 4.1 Cross-section showing sand bed with multiple number of reinforcement



Figure 4.2 Placement of geogrid during experiment

4.3 EQUIPMENT SETUP

After preparation of reinforced or unreinforced sample, footing is placed over the top of sand bed in such a way so that footing is parallel to the wall of test tank. Proving ring of desired capacity is attached with the cylindrical shaft of static loading unit and brought into contact with footing through metallic ball in between shaft and footing. Before making contact between shaft and footing, ensure that shaft is vertical. Two dial gauge of same specification is placed at the diagonally opposite corner of the footing. The whole setup of equipment is shown in Figure 4.2.



Figure 4.3 Equipment setup

4.4 MODEL TEST PROCEDURE

Theoretical bearing capacity of the sand bed is calculated using Meyerhof's bearing capacity formula. Now this ultimate load is applied on the footing in 8 steps. Load to be applied in one steps is calculate by dividing the ultimate load by number of steps and then load in one step is again dividing by least count of proving ring used during the test to calculate the number of division in each step. Since the test is stress controlled, the load calculated in one step is applied on the footing and corresponding settlement is measured by taking average reading of both dial gauge fitted at two diagonally opposite corner of footing. After taking the reading on proving ring and dial gauge, load applied is calculated by multiplying the number of division on proving ring by it's least count and corresponding settlement is calculated by multiplying the dial gauge reading by it's least count i.e. 0.01. Now the load-settlement curve is drawn and using double tangent method, experimental bearing capacity is extracted.

4.5 MODEL TEST SERIES

Total 32 number of tests is performed with varying number of geogrid layers, eccentricity and footing size as shown in Table 4.1.

Table 4.1. The sequence of the model test series

Number of Test	Number of Geogrid Layer (N)	B/L	e/B
1 - 8	0	0.5, 0.33	0.00, 0.05, 0.10, 0.15
9 - 16	2	0.5, 0.33	0.00, 0.05, 0.10, 0.15
16 - 24	3	0.5, 0.33	0.00, 0.05, 0.10, 0.15
24 - 32	4	0.5, 0.33	0.00, 0.05, 0.10, 0.15

RESULTS AND ANALYSIS

5.1 GENERAL

Load tests have been performed on model rectangular footings of size $10\text{cm} \times 20\text{cm}$ and $10\text{cm} \times 30\text{cm}$ resting over unreinforced as well as reinforced sand bed with eccentricity varying from 0.0 to $0.15B$. For preparing reinforced sand bed, multiple number (2, 3, 4) of geogrid (SS20) layers have been introduced. Settlement corresponding to each load increment is noted and the test result is plotted in term of load-settlement curve. Ultimate bearing capacity for each test is determined from load-settlement curve using tangent intersection method. Bearing capacity result is then analyzed to develop mathematical relationship for reduction factor (R_{KR}) which is the function of eccentricity width ratio (e/B) and the ratio of depth of reinforcement layer and width of footing (d_f/B).

5.2 BEARING CAPACITY OF UNREINFORCED SAND

5.2.1 MODEL TEST RESULT

Results of load test have been plotted in term of load-settlement curve as shown in Figure 5.1 & 5.2 for footing size $10 \times 20\text{cm}$ ($B/L = 0.5$) and $10 \times 30\text{cm}$ ($B/L = 0.33$) respectively. From the graph, it is observed that ultimate bearing capacity decreases as eccentricity width ratio (e/B) increases and also the total settlement at failure load decreases as eccentricity width ratio (e/B) increases. By comparing the graph shown in Figure 5.1 and Figure 5.2, it can also be concluded that as the width to length ratio (B/L) decreases, load carrying capacity of footing increases.

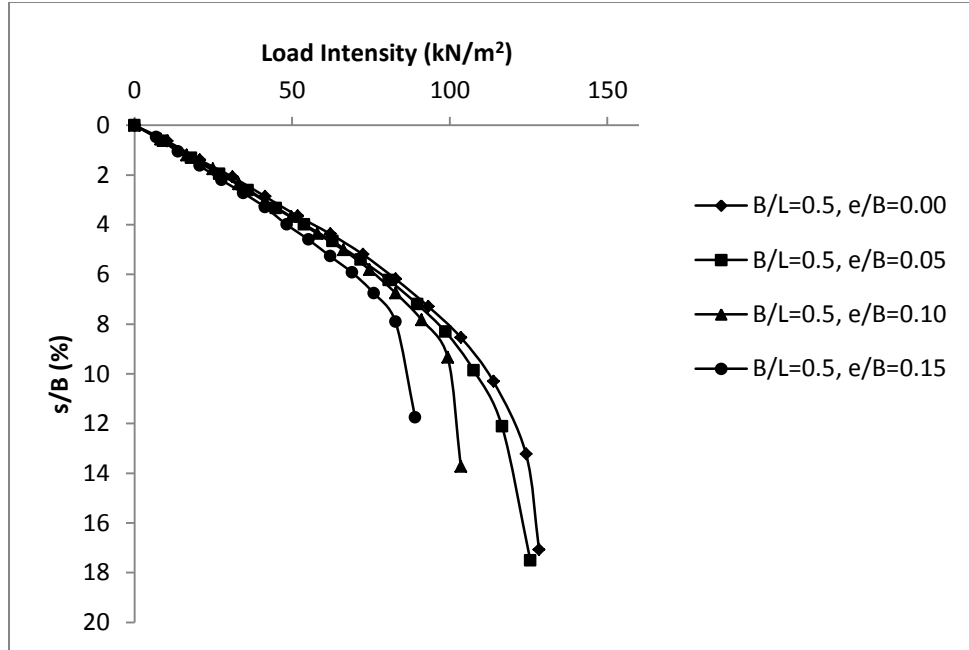


Figure 5.1. Load-settlement curve of unreinforced sand bed ($B/L=0.5$)

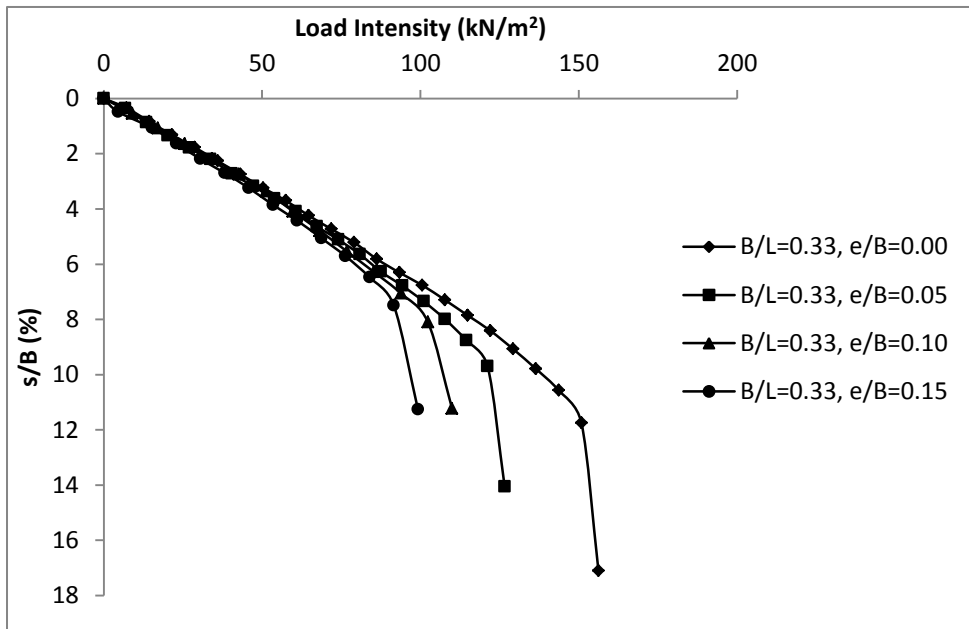


Figure 5.2. Load-settlement curve of unreinforced sand bed ($B/L=0.33$)

From the load-settlement curve shown in Figure 5.1 and Figure 5.2, ultimate load carrying capacity of both B/L ratio i.e. 0.5 & 0.33 and for all eccentricity has been calculated using

tangent intersection method. The result has been tabulated in Table 5.1 & 5.2 for $B/L=0.5$ & 0.33 respectively and compared with theoretical value of load carrying capacity given by different authors. The variation of theoretical bearing capacity with eccentricity calculated by using different formula along with experimental results has been plotted in Figure 5.3 for $B/L=0.5$ and in Figure 5.4 for $B/L=0.33$.

Table 5.1. Theoretical bearing capacity of unreinforced sand bed for $B/L=0.5$

S. No	e/B	D_f/B	$\phi = 40.9^\circ$					
			Model Test q_u (kN/m ²)	Meyrhof (1953) q_u (kN/m ²)	Michalowski (1997) q_u (kN/m ²)	Vesic (1973) q_u (kN/m ²)	I.S. 6403 (1981) q_u (kN/m ²)	Hansen (1970) q_u (kN/m ²)
1	0	0	120	99.17	115.65	73.28	79.42	53.46
2	0.05	0	105	87.79	104.77	67.59	71.47	49.24
3	0.1	0	90	76.12	91.52	61.57	63.54	44.83
4	0.15	0	75	69.94	78.67	55.13	55.59	40.22

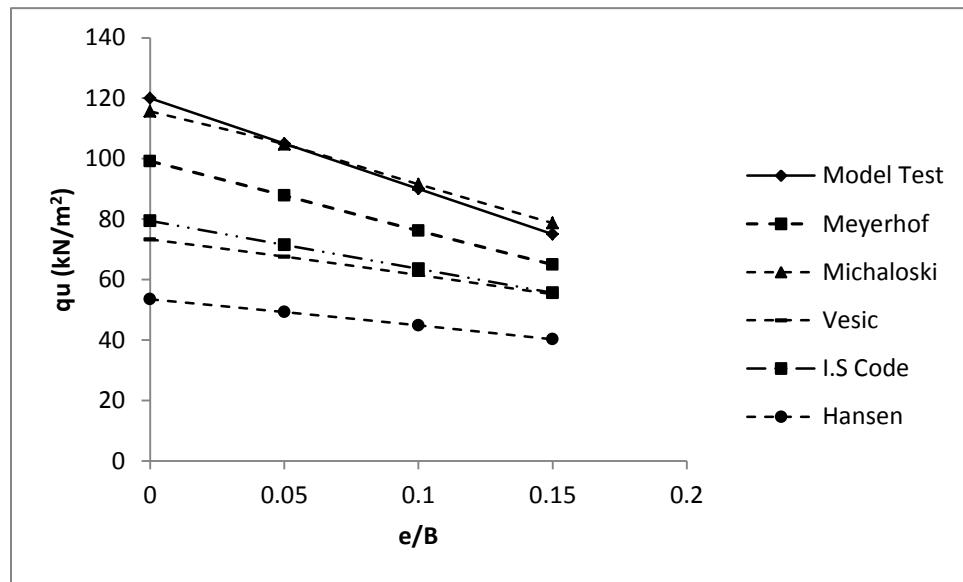


Figure 5.3. Variation in q_u with e/B ($B/L=0.5$)

Table 5.2. Theoretical bearing capacity of unreinforced sand bed for B/L=0.33

S. No	e/B	D_f/B	$\phi = 40.9^\circ$					
			Model Test q_u (kN/m ²)	Meyrhof (1953) q_u (kN/m ²)	Michalowski (1997) q_u (kN/m ²)	Vesic (1973) q_u (kN/m ²)	I.S. 6403 (1981) q_u (kN/m ²)	Hansen (1970) q_u (kN/m ²)
1	0	0	125	92.83	111.45	79.65	86.37	58.07
2	0.05	0	110	82.1	98.51	72.49	77.73	52.87
3	0.1	0	94	72.34	85.97	65.13	69.09	47.57
4	0.15	0	80	62.18	73.14	58.27	60.45	42.57

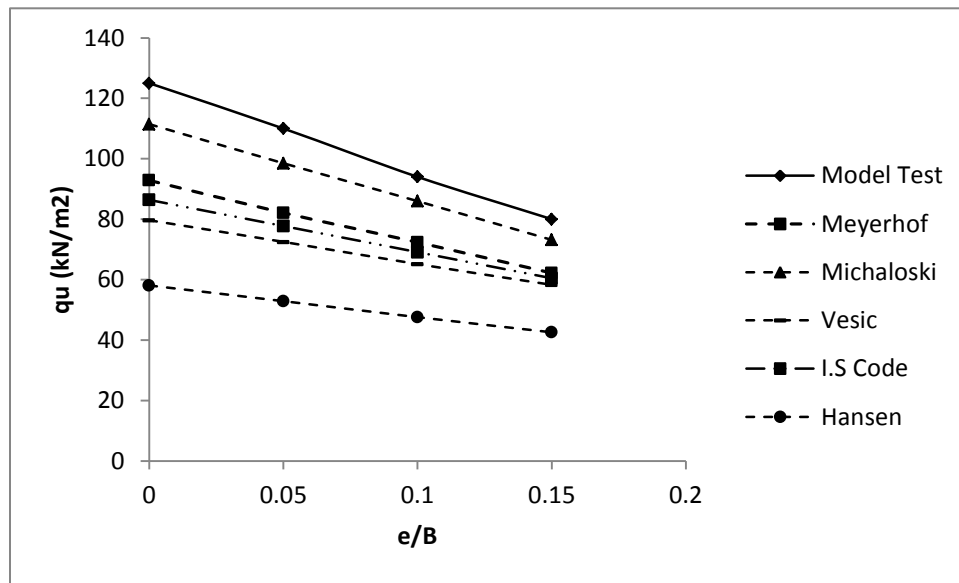


Figure 5.4. Variation in q_u with e/B (B/L=0.33)

From the bearing capacity value tabulated in Table 5.1 and Table 5.2, it is observed that the theoretical values using various formulae available in literature is widely varying. However, experimental value of bearing capacity is more than theoretical values calculated using formula proposed by Michalowski (1997). Many researchers like Balla 1962, Bolt 1982, Cichy et al.

1978, Ingra and Baecher 1983 and some others have reported that experimental load carrying capacity of model footing is much higher than those calculated by traditional methods.

DeBeer (1965) collected a number of bearing capacity test results and calculated the N_γ value for all bearing capacity value. The change in N_γ for small scale test and large scale test has been compared by DeBeer (1965) as shown in Figure 5.5.

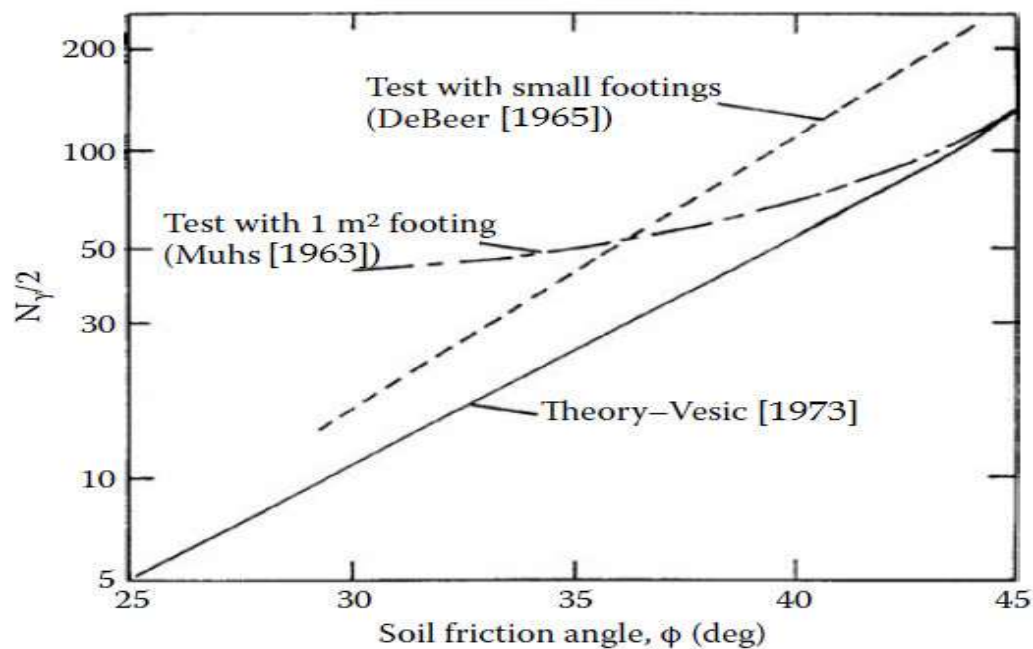


Figure 5.5. Change in N_γ with ϕ for different size of footing

(Source: Shallow Foundation, 7th Edition, B. M. Das)

The N_γ vs ϕ plot is showing that as the internal friction angle of foundation soil increasing, difference between theoretical N_γ value calculated by Vesic (1973) and experimental N_γ value calculated by DeBeer (1965) by performing small model footing test is increases. In this research work the value of internal friction angle ϕ is 40.9 for which difference in theoretical and

experimental N_γ value is large as shown in Figure 5.5. The effect of higher ϕ value can also be observed in the ultimate bearing capacity result obtained in the present work.

Laboratory model test result tabulated in Table 5.1 and Table 5.2 shows that as B/L ratio decreases, load carrying capacity of the footing increases. The result of both the footings has been plotted in figure 5.6 to 5.9 for two different B/L ratios at same e/B same to show the effect of B/L ratio.

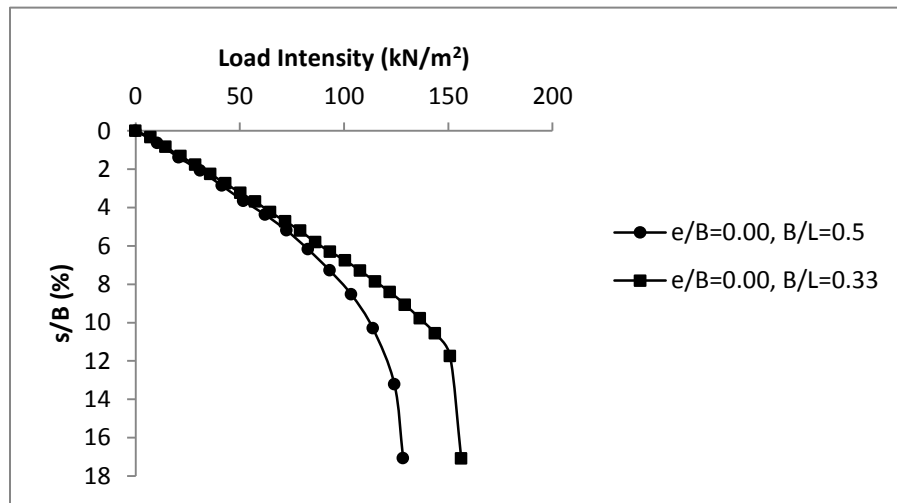


Figure 5.6. Load-settlement curve of unreinforced sand for $e/B=0.00$ and different B/L ratio

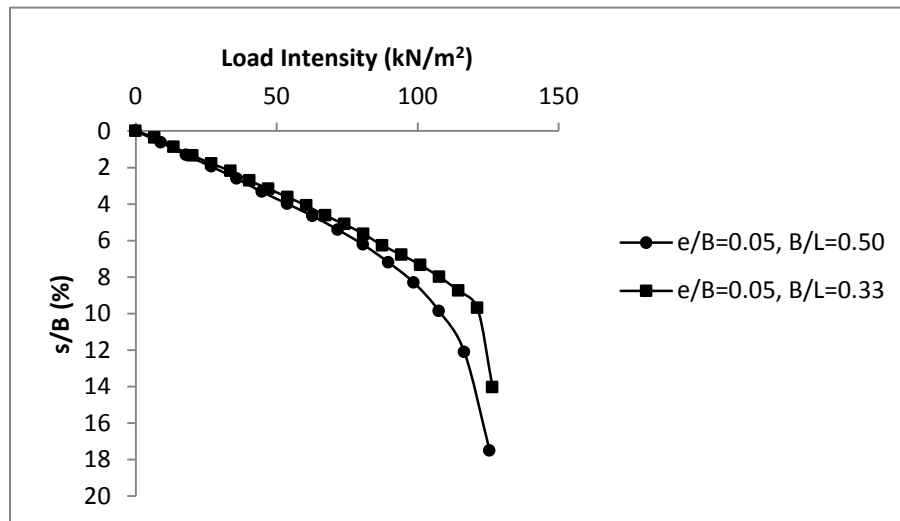


Figure 5.7. Load-settlement curve of unreinforced sand for $e/B=0.05$ and different B/L ratio

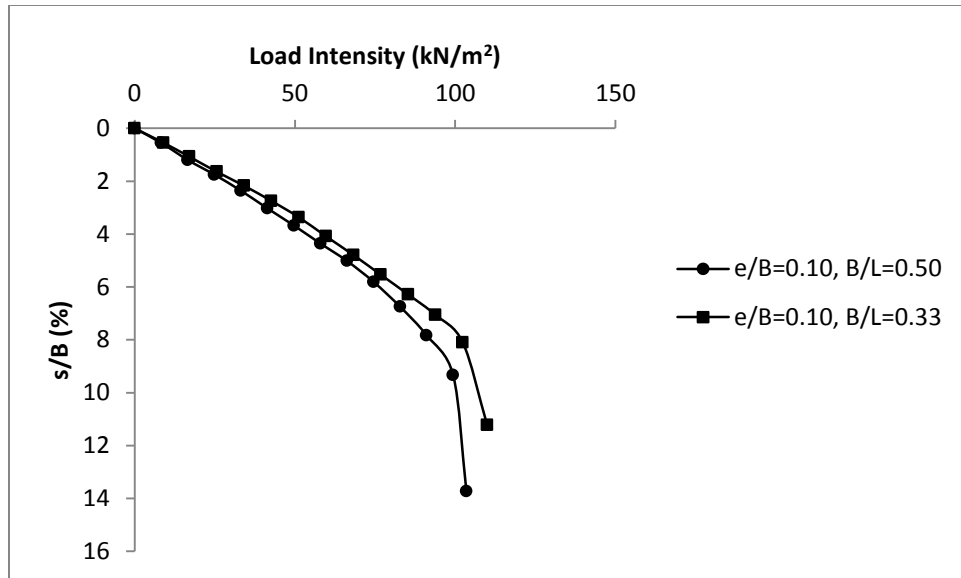


Figure 5.8. Load-settlement curve of unreinforced sand for $e/B=0.10$ and different B/L ratio

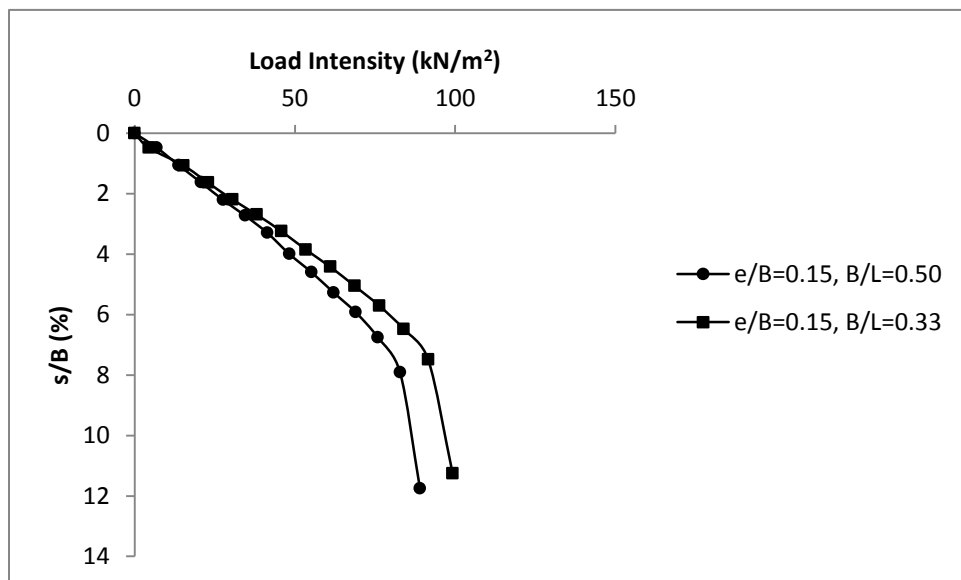


Figure 5.9. Load-settlement curve of unreinforced sand for $e/B=0.15$ and different B/L ratio

5.3 BEARING CAPACITY OF GEOGRID REINFORCED SAND

5.3.1 MODEL TEST RESULT

Laboratory model tests have been performed using rectangular footing with $B/L=0.5$ & 0.33 resting over the geogrid reinforced sand. The sand is reinforced by placing multilayer ($N=2, 3, 4$) geogrids with d_f/B ratio equals to $0.6, 0.85$ & 1.1 , where d_f is the depth of lower most geogrid layer from bottom of footing and B is the width of footing. The load is applied centrally as well as eccentrically on the model footing using static loading machine. Settlement corresponding to each load increment has been noted down and load settlement curve has been plotted. The ultimate bearing capacity has been found from load-settlement curve using tangent intersection method. Load settlement curve shown in Figure 5.10 to 5.15 is showing the effect of eccentricity on the load bearing capacity of footing on reinforced sand. From the graph it can be observed that load bearing capacity decreases with the increase in eccentricity.

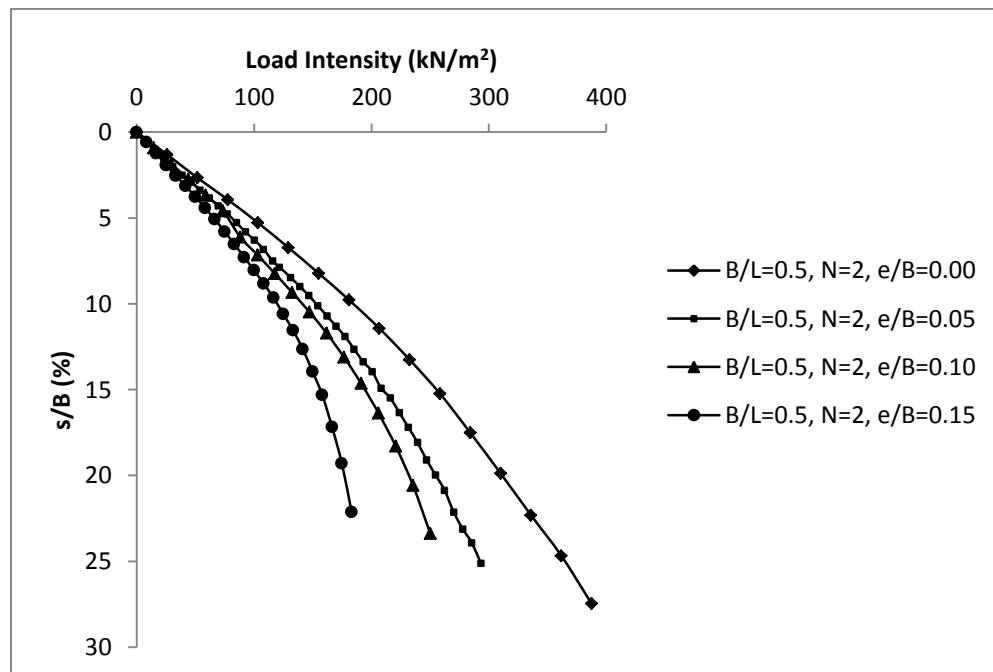


Figure 5.10. Load-settlement curve for $B/L=0.5$ & $N=2$ and different e/B ratio

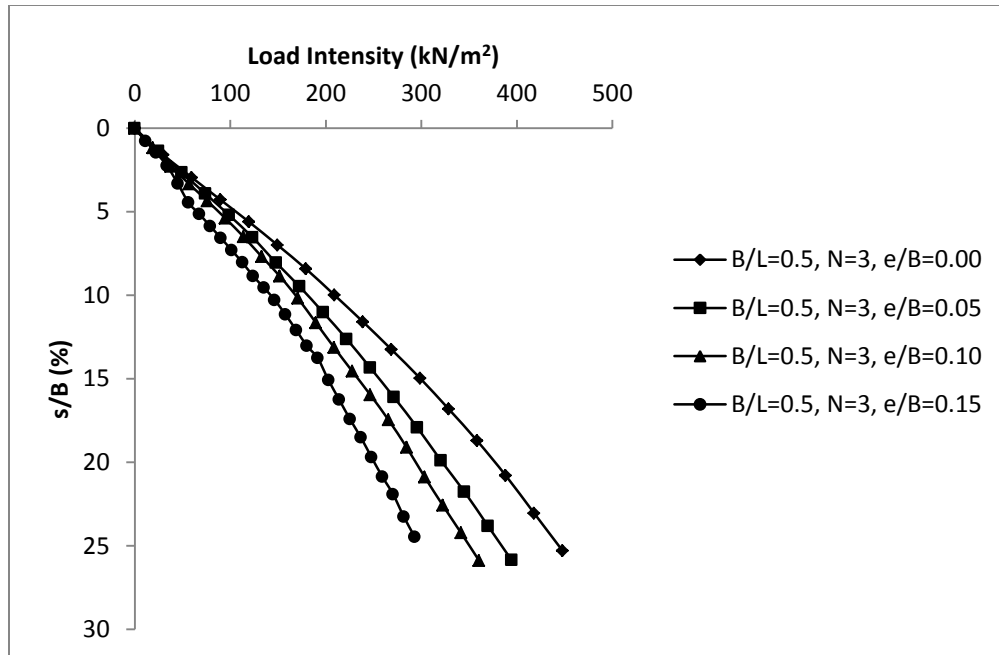


Figure 5.11. Load-settlement curve for $B/L=0.5$ & $N=3$ and different e/B ratio

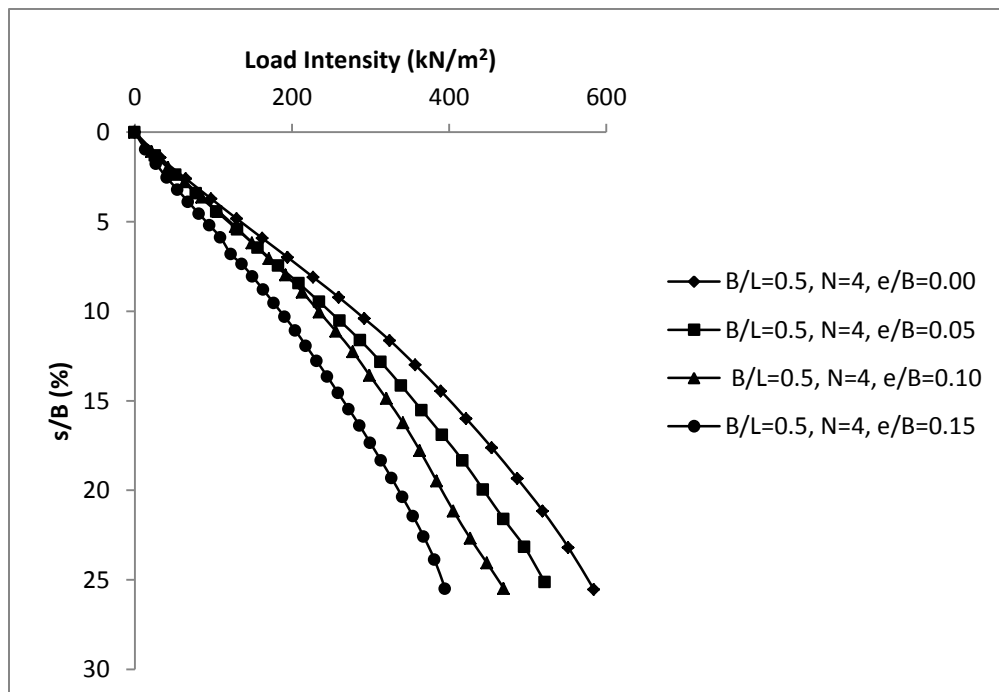


Figure 5.12. Load-settlement curve for $B/L=0.5$ & $N=4$ and different e/B ratio

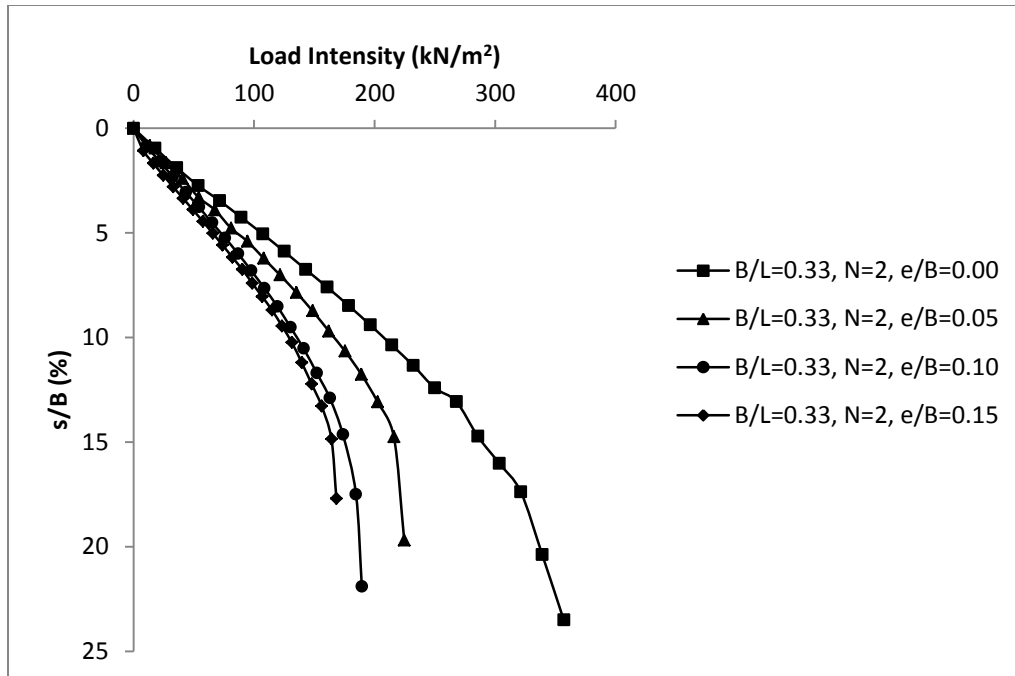


Figure 5.13. Load-settlement curve for $B/L=0.33$ & $N=2$ and different e/B ratio

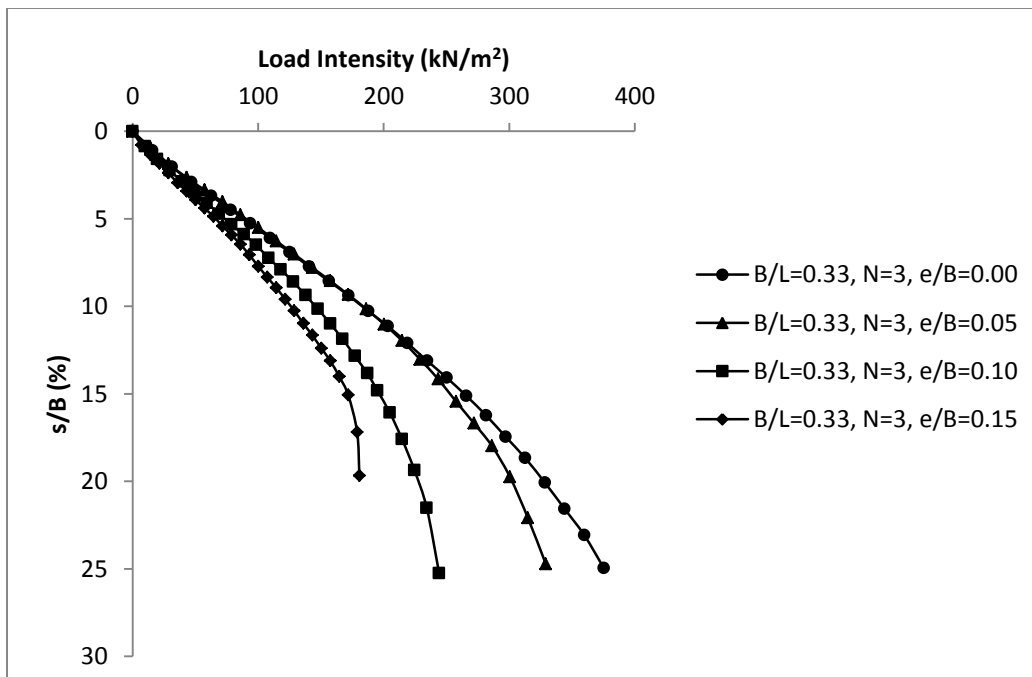


Figure 5.14. Load-settlement curve for $B/L=0.33$ & $N=3$ and different e/B ratio

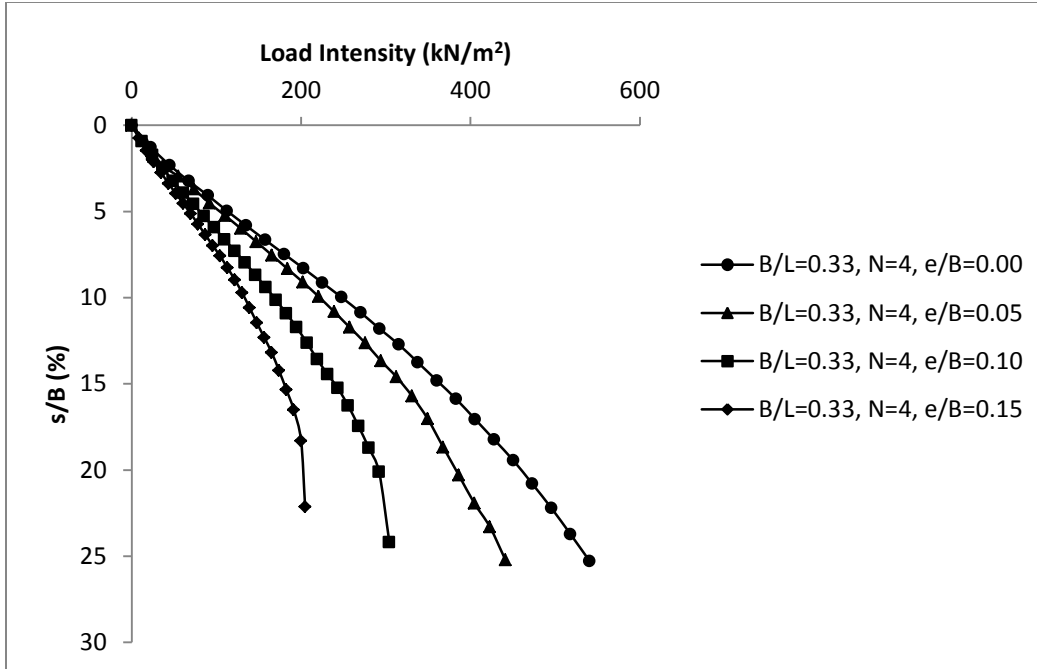


Figure 5.15. Load-settlement curve for $B/L=0.33$ & $N=4$ and different e/B ratio

Load settlement curves with varying number of geogrid layers have been plotted in Figure 5.16 to 5.23 to show the effect of reinforcement layer with constant eccentricity width (e/B) ratio and width to length (B/L) ratio.

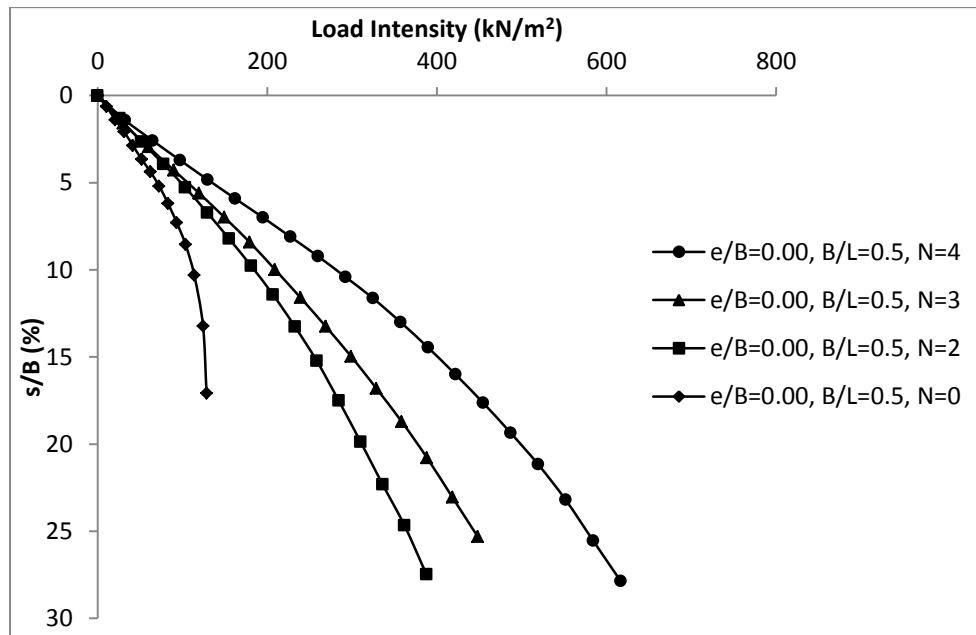


Figure 5.16. Load-settlement curve for $B/L=0.5$ & $e/B=0.00$ with different N

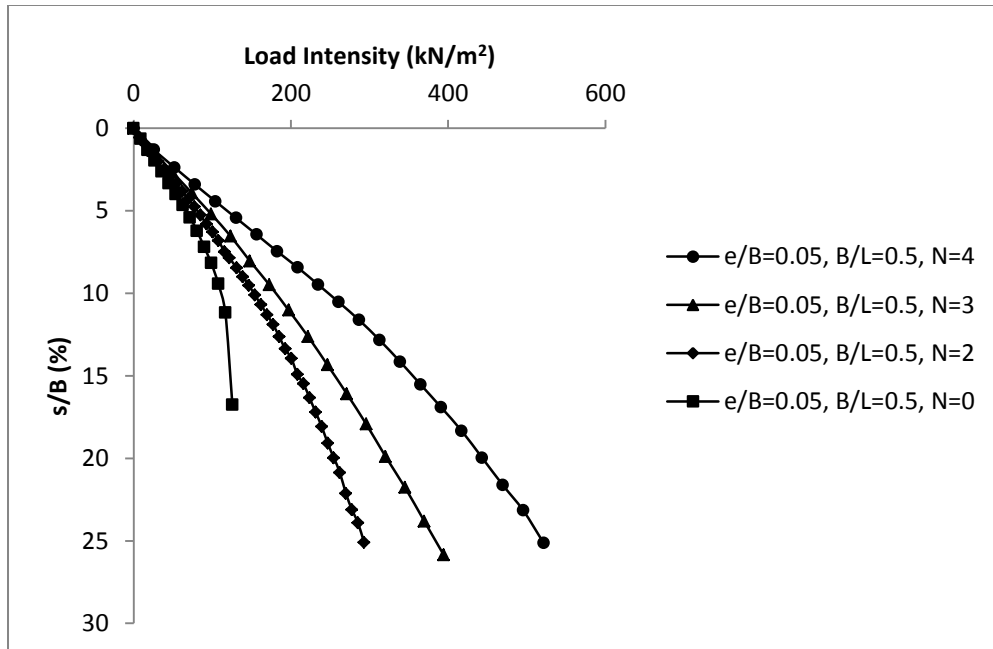


Figure 5.17. Load-settlement curve for $B/L=0.5$ & $e/B=0.05$ with different N

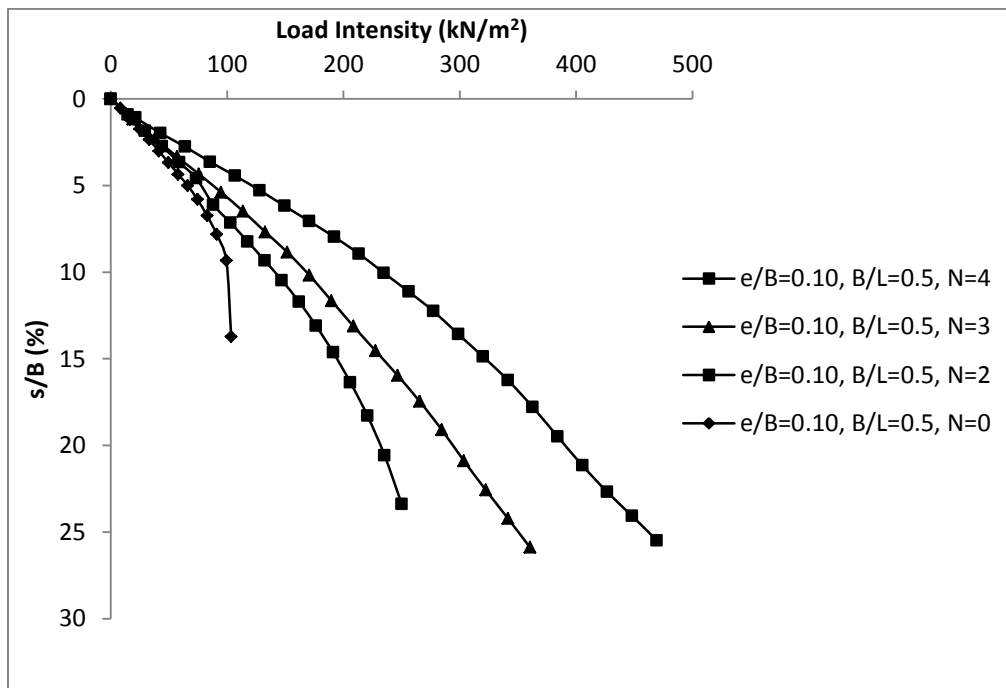


Figure 5.18. Load-settlement curve for $B/L=0.5$ & $e/B=0.10$ with different N

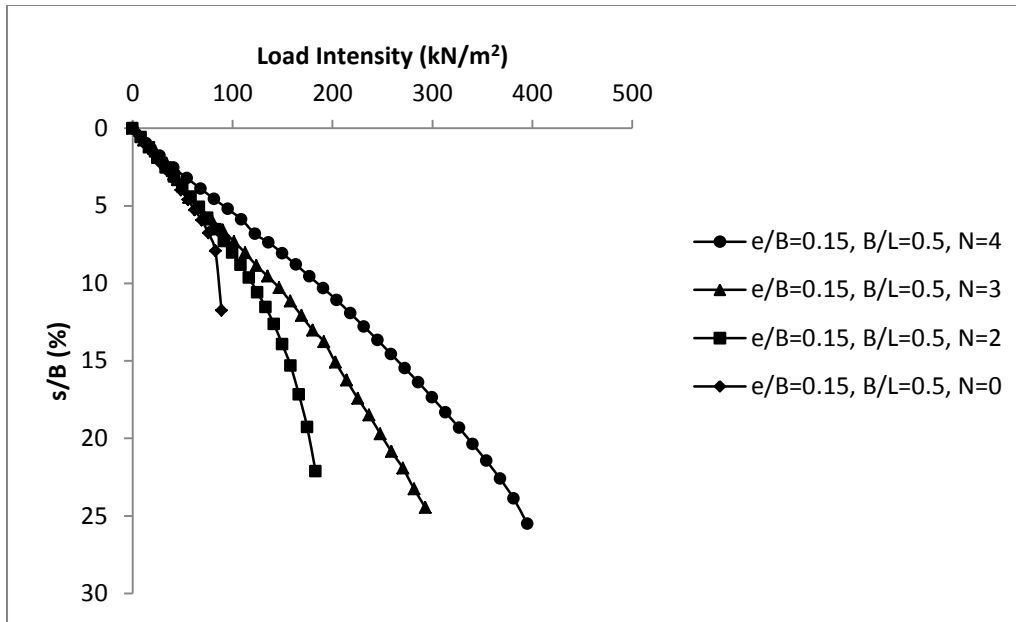


Figure 5.19. Load-settlement curve for $B/L=0.5$ & $e/B=0.15$ with different N

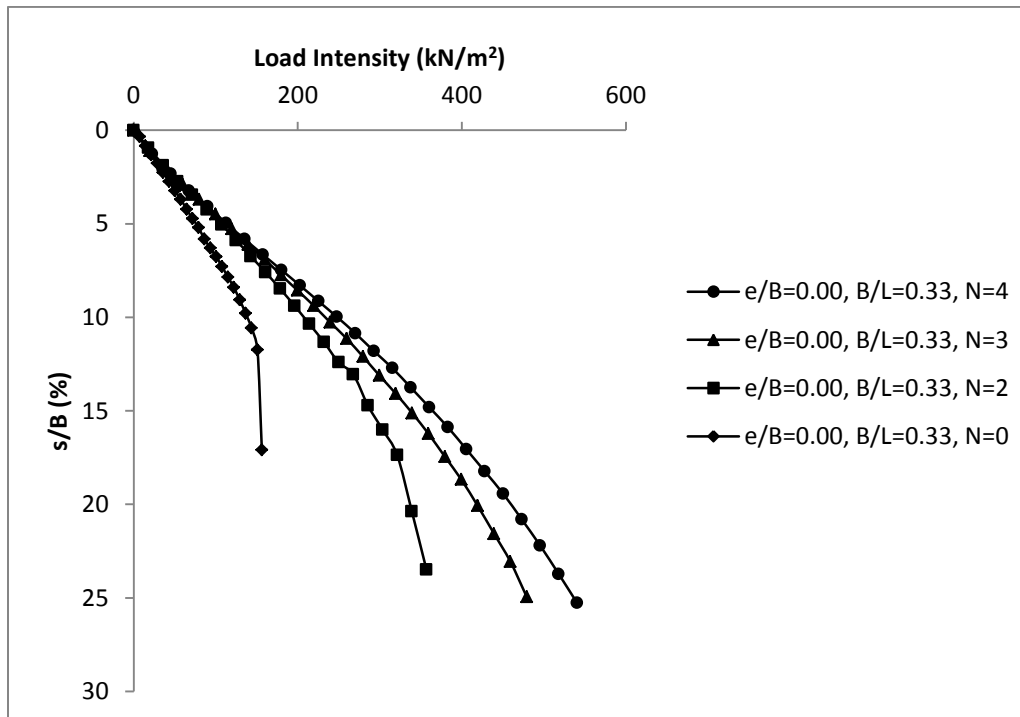


Figure 5.20. Load-settlement curve for $B/L=0.33$ & $e/B=0.00$ with different N

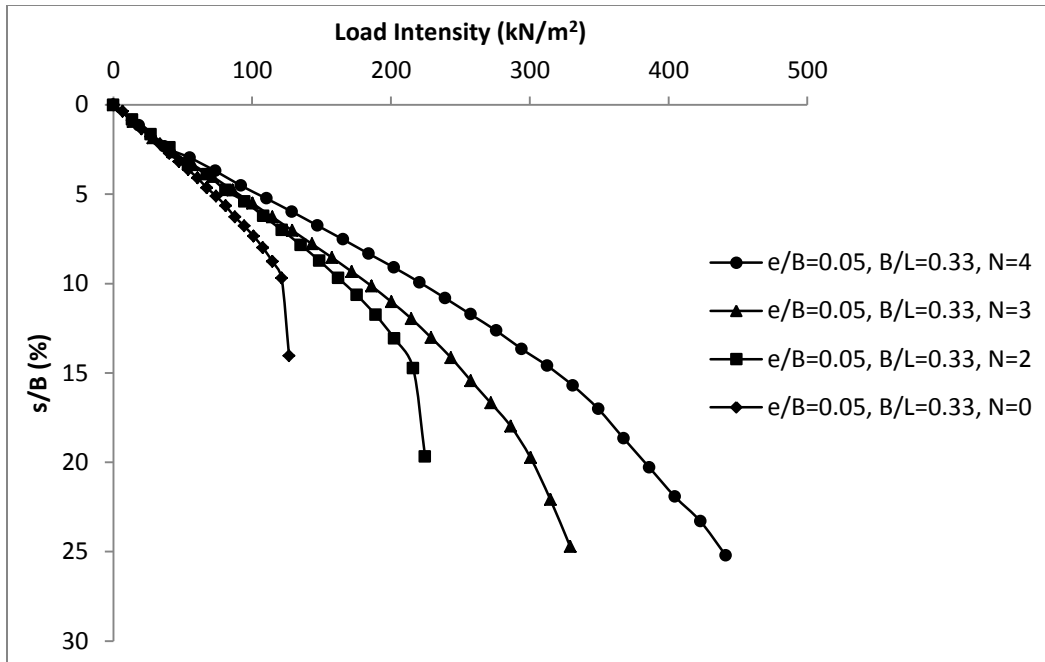


Figure 5.21. Load-settlement curve for $B/L=0.33$ & $e/B=0.05$ with different N

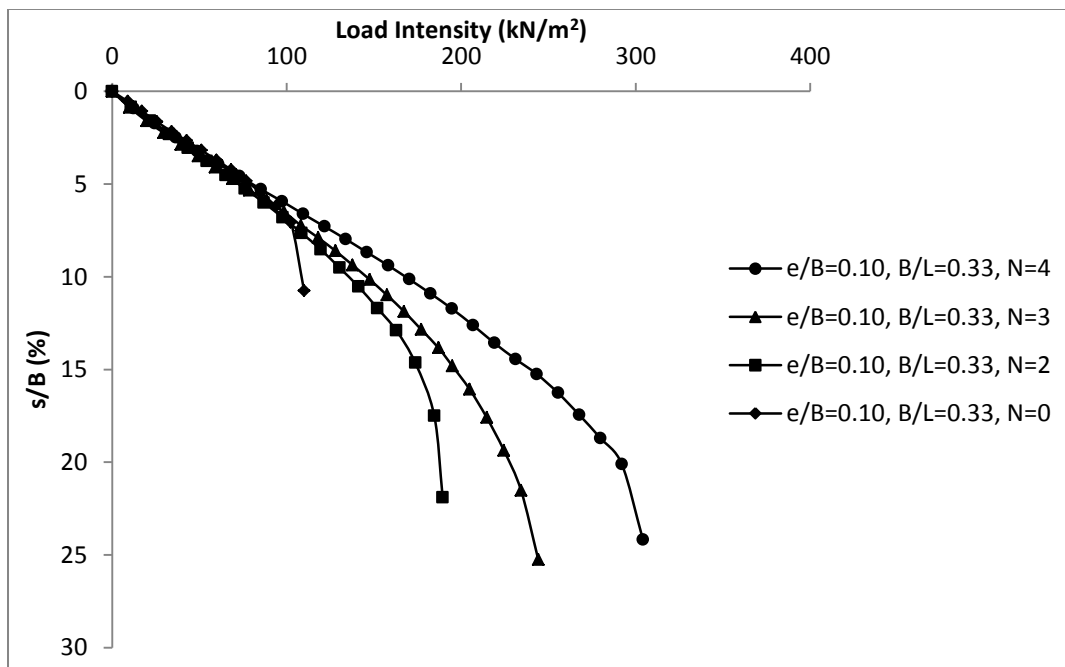


Figure 5.22. Load-settlement curve for $B/L=0.33$ & $e/B=0.10$ with different N

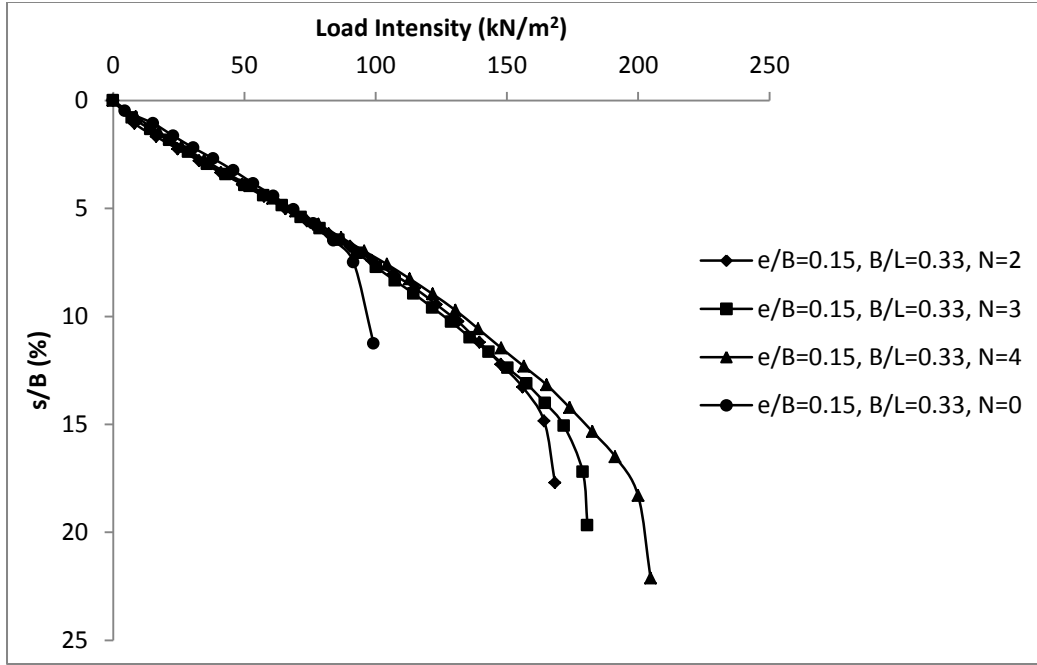


Figure 5.23. Load-settlement curve for $B/L=0.33$ & $e/B=0.15$ with different N

From the load-settlement curve shown in Figure 5.10 to Figure 5.15, ultimate load carrying capacity of both B/L ratio (i.e. 0.33 & 0.5) and for all eccentricity has been calculated using tangent intersection method. The result has been tabulated in Table 5.3 to Table 5.6 for $e/B = 0$, 0.05, 0.10 & 0.15 respectively with different number of geogrid layers. Theoretical ultimate bearing capacity for centrally loaded footing on reinforced sand has been calculated using formula given by Huang and Menq (1997) as shown in equation 5.1. This formulae reported by Huang and Menq (1997) corresponds to strip footing. A shape factor for rectangular footings on reinforced soil has been multiplied as per Huang and Menq (2000).

$$q_{uR(e=0)} = \left[0.5 - 0.1 \left(\frac{B}{L} \right) \right] (B + \Delta B) \gamma B N_{\gamma} + \gamma d N_q \quad (5.1)$$

For the calculation of ultimate load carrying capacity of eccentrically loaded foundation on reinforced soil, the reduction factor method proposed Purkayastha and Char (1977) for the case of un-reinforced soil has been extended. The relationship can be written in line with Purkayastha and Char (1977) as shown in equation 5.2.

$$\frac{q_{uR(e)}}{q_{uR(e=0)}} = 1 - R_{KR} \quad (5.2)$$

Where, $q_{uR(e)}$ is the ultimate bearing capacity of reinforced sand under eccentric loading; q_{uR} is the ultimate bearing capacity of reinforced sand under centric loading and R_{KR} is the reduction factor. Patra et. al. (2006) proposed reduction factor (R_{KR}) for strip footing on reinforced soil in as shown in equation 5.3.

$$R_{KR} = 4.97 \left(\frac{d_f}{B} \right)^{-0.12} \left(\frac{e}{B} \right)^{1.21} \quad (5.3)$$

Table 5.3. Bearing capacity of reinforced sand bed for $e/B = 0$

e/B=0			
N	B/L	$q_{uR(th)}$ (Huang & Menq, 1997) (kN/m²)	$q_{uR(exp)}$ (kN/m²)
2	0.33	198.16	225
	0.5	193.25	220
3	0.33	245.25	275
	0.5	239.36	270
4	0.33	292.33	380
	0.5	285.96	365

Table 5.4. Bearing capacity of reinforced sand bed for $e/B = 0.05$

$e/B=0.05$			
N	B/L	$q_{uR(th)}$ (Huang & Menq, 1997) (kN/m²)	$q_{uR(exp)}$ (kN/m²)
2	0.33	170.59	201
	0.5	166.57	198
3	0.33	211.89	242
	0.5	207.97	238
4	0.33	254.56	323
	0.5	248.97	314

Table 5.5. Bearing capacity of reinforced sand bed for $e/B=0.10$

$e/B=0.10$			
N	B/L	$q_{uR(th)}$ (Huang & Menq, 1997) (kN/m²)	$q_{uR(exp)}$ (kN/m²)
2	0.33	134.59	171
	0.5	131.45	165
3	0.33	169.71	195
	0.5	165.78	189
4	0.33	204.05	251
	0.5	200.12	237

Table 5.6 Bearing capacity of reinforced sand bed for $e/B=0.15$

$e/B=0.15$			
N	B/L	$q_{uR(th)}$ (Huang & Menq, 1997) (kN/m²)	$q_{uR(exp)}$ (kN/m²)
2	0.33	94.17	140
	0.5	91.82	132
3	0.33	121.93	151
	0.5	119.19	140
4	0.33	149.1	182
	0.5	146.16	164

5.4 ANALYSIS OF TEST RESULT

The ultimate bearing capacity of reinforced sand for both cases i.e. $B/L=0.33$ and 0.5 with different values of e/B and N has been tabulated in Table 5.7 and Table 5.8. Using the experimental ultimate bearing capacity calculated from load-settlement curve, the ratio $q_{uR(e)}/q_{uR}$ has been calculated for each case. The reduction factor R_{KR} is then calculated for each case by using Equation 5.2 and tabulated in Table 5.7 and Table 5.8.

Empirical relation for reduction factor (R_{KR}) proposed by Patra et. al. (2006) for strip footing shows that R_{KR} is the function of d_f/B and e/B and may be expressed as

$$R_{KR} = \alpha_1 \left(\frac{d_f}{B} \right)^{\alpha_2} \left(\frac{e}{B} \right)^{\alpha_3} \quad (5.4)$$

Where $\alpha_1, \alpha_2, \alpha_3$ are dimensionless constants.

The purpose of the present study is to find out the coefficient $\alpha_1, \alpha_2, \alpha_3$ for rectangular footing by conducting a number of laboratory model tests using rectangular footing with $B/L=0.5$ & 0.33 resting over multi-layered geogrid reinforced sand bed.

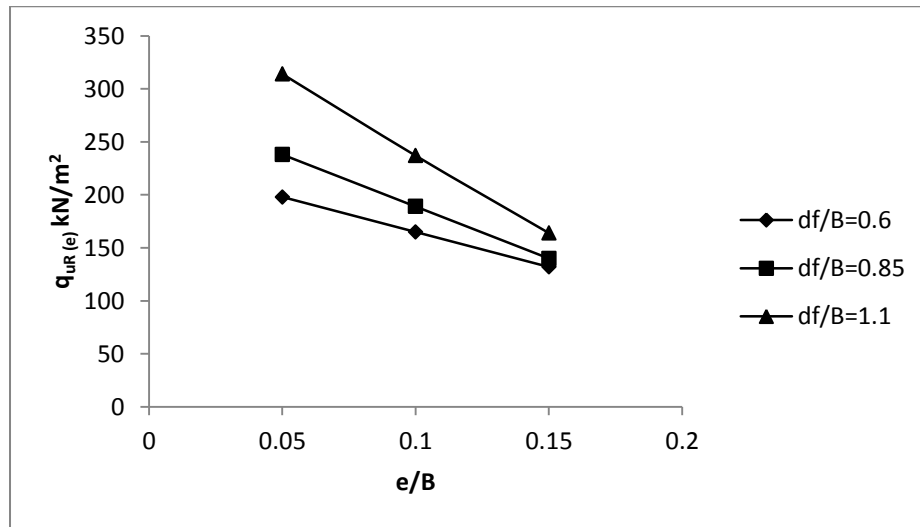
5.4.1 ANALYSIS OF RECTANGULAR FOOTING WITH $B/L=0.5$

Table 5.7 Experimental reduction factor for eccentrically loaded footing resting on reinforced sand bed with $B/L=0.5$

$\frac{B}{L}$	$\frac{d_f}{B}$	$\frac{e}{B}$	$q_{uR(e)} \text{ (kN/m}^2\text{)}$	$\frac{q_{uR(e)}}{q_{uR(e=0)}}$	$R_{KR} = 1 - \frac{q_{uR(e)}}{q_{uR(e=0)}}$
0.5	0.6	0.05	198	0.90	0.10
0.5	0.6	0.10	165	0.75	0.25
0.5	0.6	0.15	132	0.60	0.40

Table 5.7 (Continued)

$\frac{B}{L}$	$\frac{d_f}{B}$	$\frac{e}{B}$	$q_{uR(e)}$ (kN/m ²)	$\frac{q_{uR(e)}}{q_{uR(e=0)}}$	$R_{KR} = 1 - \frac{q_{uR(e)}}{q_{uR(e=0)}}$
0.5	0.85	0.05	238	0.88	0.12
0.5	0.85	0.10	189	0.70	0.30
0.5	0.85	0.15	140	0.51	0.49
0.5	1.1	0.05	314	0.86	0.14
0.5	1.1	0.10	237	0.65	0.35
0.5	1.1	0.15	164	0.45	0.55

Figure 5.24. Variation of $q_{uR(e)}$ with e/B for $B/L=0.5$

First of all, value of α_2 has been calculated using R_{KR} vs d_f/B curve as shown in Figure 5.25 and

α_3 using R_{KR} vs e/B curve plotted on log-log graph as shown in Figure 5.26.

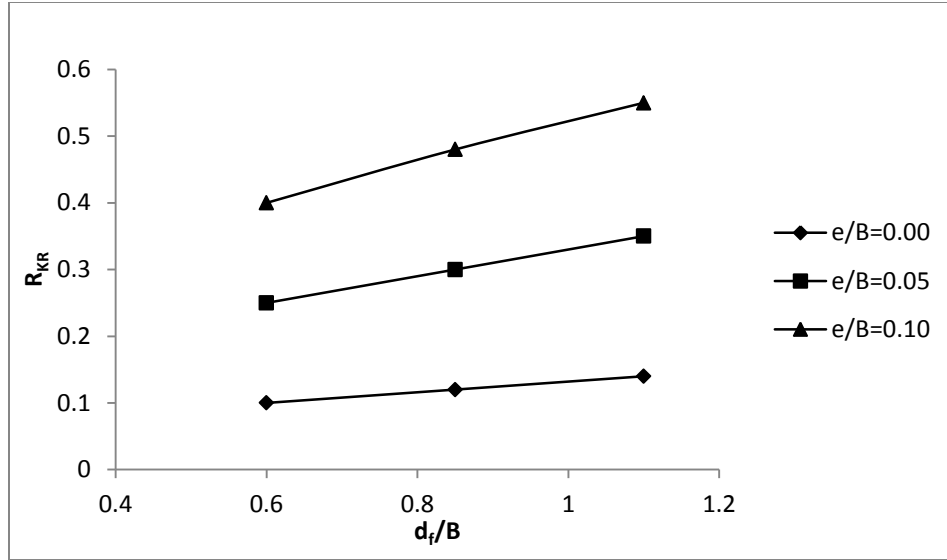


Figure 5.25. Variation of R_{KR} with d_f/B for $B/L=0.5$

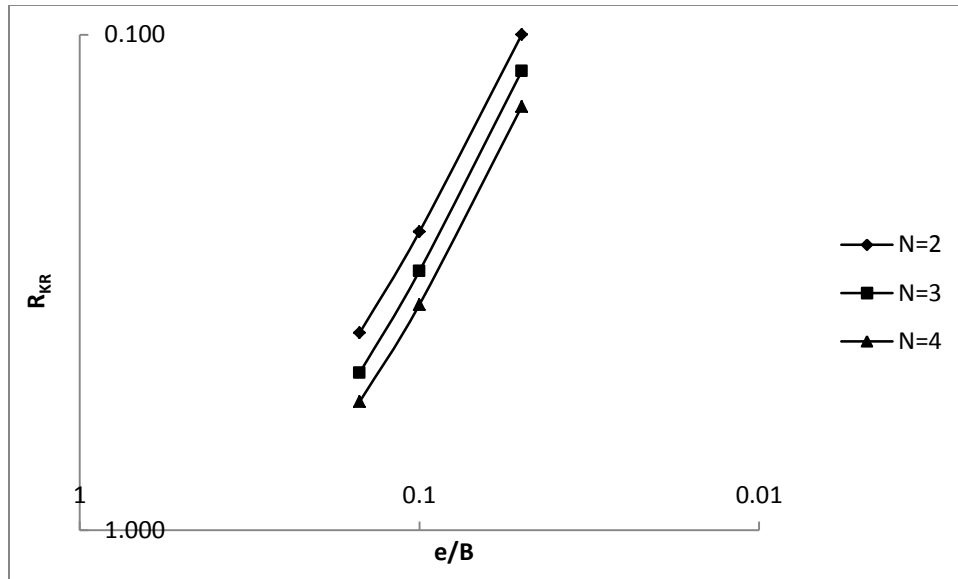


Figure 5.26. Variation of R_{KR} with e/B for $B/L=0.5$

From the Figure 5.25, α_2 value has been calculated from R_{KR} vs d_f/B curve which is the average slope of all the line. The value of α_2 has been found as 0.555.

$$R_{KR} \alpha \left(\frac{d_f}{B} \right)^{0.555} \quad (5.5)$$

From the Figure 5.26, α_3 value has been calculated from R_{KR} vs e/B curve which is the average slope of all the line. The value of α_3 has been found as 1.261.

$$R_{KR} \alpha \left(\frac{e}{B} \right)^{1.26} \quad (5.6)$$

By combining Equation 5.5 and 5.6, equation for reduction factor as shown in Equation 5.4 may be written as

$$R_{KR} = \alpha_1 \left(\frac{d_f}{B} \right)^{0.555} \left(\frac{e}{B} \right)^{1.26} \quad (5.7)$$

Now the value of α_1 will be calculated for each e/B ratio and one d_f/B and corresponding R_{KR} value by using Equation 5.7 and then the average value is taken as α_1 .

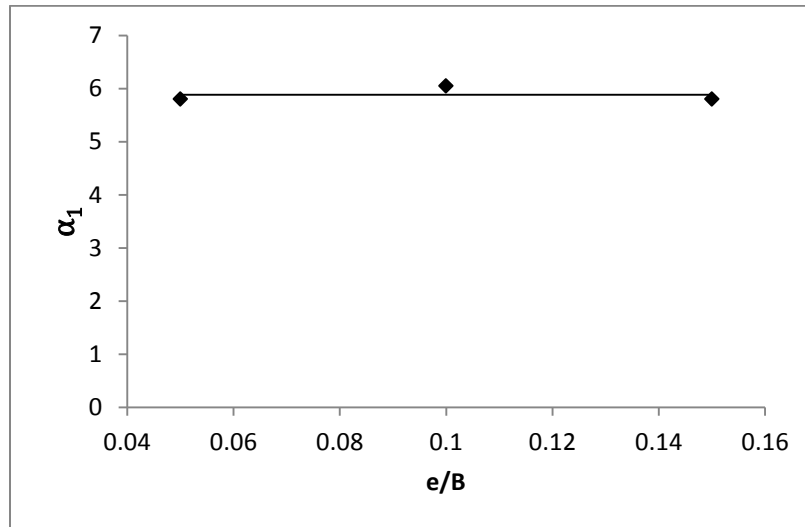


Figure 5.27 Variation of α_1 with e/B for $B/L=0.5$

The average value of α_1 from the Figure 5.27 has been found out as 5.88. So the final equation for reduction factor for the footing with $B/L=0.5$ can be written as shown in equation 5.8.

$$R_{KR} = 5.88 \left(\frac{d_f}{B} \right)^{0.555} \left(\frac{e}{B} \right)^{1.26} \quad (5.8)$$

5.4.2 ANALYSIS OF RECTANGULAR FOOTING WITH B/L=0.33

Same procedure has been followed to derive the empirical relation for reduction factor for footing with $B/L=0.33$.

Table 5.8 Experimental reduction factor for eccentrically loaded footing resting on reinforced sand bed with B/L=0.33

$\frac{B}{L}$	$\frac{d_f}{B}$	$\frac{e}{B}$	$q_{uR(e)} \text{ (kN/m}^2\text{)}$	$\frac{q_{uR(e)}}{q_{uR(e=0)}}$	$R_{KR} = 1 - \frac{q_{uR(e)}}{q_{uR(e=0)}}$
0.33	0.6	0.05	201	0.89	0.11
0.33	0.6	0.10	171	0.76	0.24
0.33	0.6	0.15	140	0.62	0.38
0.33	0.85	0.05	242	0.88	0.12
0.33	0.85	0.10	195	0.71	0.29
0.33	0.85	0.15	151	0.55	0.45
0.33	1.1	0.05	323	0.85	0.15
0.33	1.1	0.10	251	0.66	0.34
0.33	1.1	0.15	182	0.48	0.52

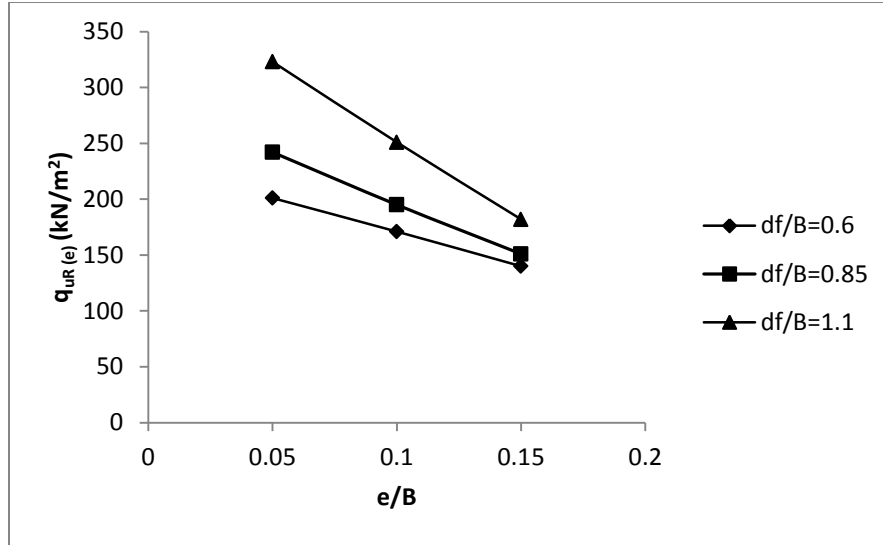


Figure 5.28. Variation of $q_{uR(e)}$ with e/B for $B/L=0.33$

Value of α_2 has been calculated using R_{KR} vs d_f/B curve as shown in Figure 5.29 and α_3 using R_{KR} vs e/B curve plotted on log-log graph as shown in Figure 5.30.

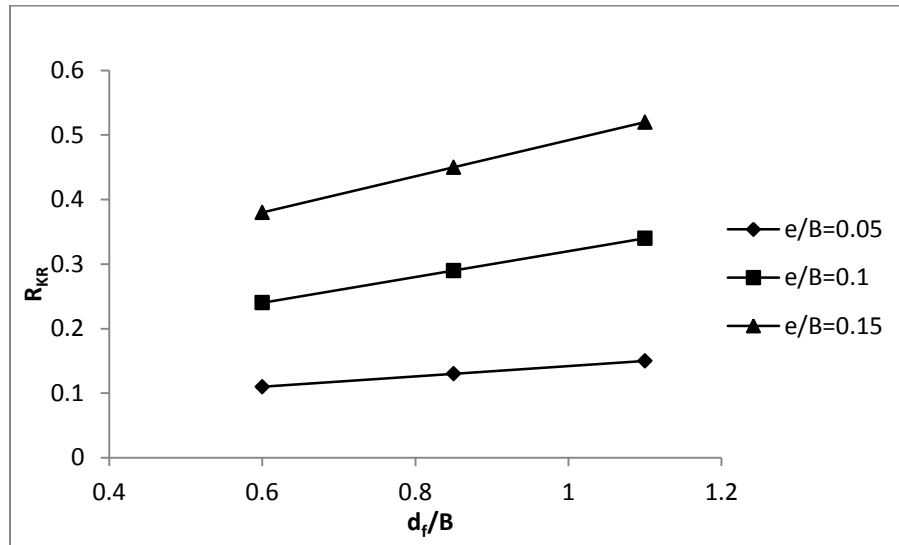


Figure 5.29. Variation of R_{KR} with d_f/B for $B/L=0.33$

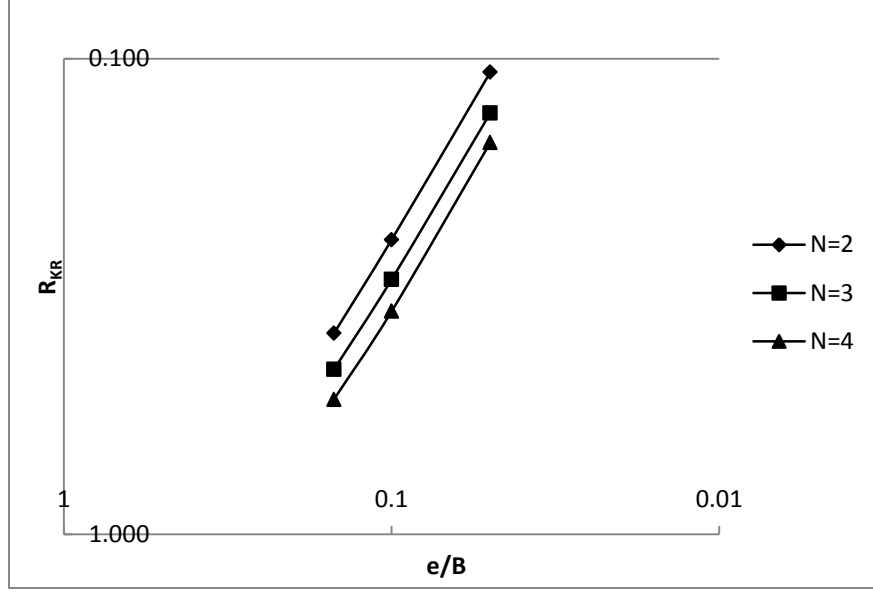


Figure 5.30 Variation of R_{KR} with e/B for $B/L=0.33$

From the Figure 5.29, α_2 value has been calculated from R_{KR} vs d_f/B curve which is the average slope of all the line. The value of α_2 has been found as 0.512. From the Figure 5.30, α_3 value has been calculated from R_{KR} vs e/B curve which is the average slope of all the line. The value of α_3 has been found as 1.13.

Now the equation for reduction factor may be written as

$$R_{KR} = \alpha_1 \left(\frac{d_f}{B} \right)^{0.512} \left(\frac{e}{B} \right)^{1.13} \quad (5.9)$$

Value of α_1 will be calculated for each e/B ratio and one d_f/B and corresponding R_{KR} value by using Equation 5.9 and then the average value is taken as α_1 .

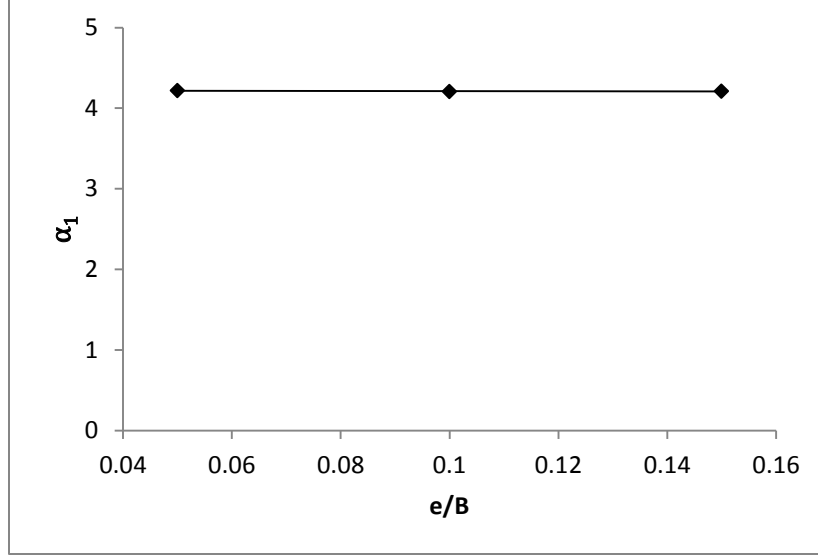


Figure 5.31 Variation of α_1 with e/B for $B/L=0.33$

The average value of α_1 from the Figure 5.31 has been found out as 4.21. So the final equation for reduction factor for the footing with $B/L = 0.33$ can be written as

$$R_{KR} = 4.21 \left(\frac{d_f}{B} \right)^{0.512} \left(\frac{e}{B} \right)^{1.13} \quad (5.10)$$

Now the Equation 5.8 and Equation 5.10 has been combined to derive a generalized reduction factor equation for rectangular footing by taking average value of α_1 , α_2 & α_3 and rounding it off to simplest form as shown in Equation 5.11.

$$R_{KR} = 5 \left(\frac{d_f}{B} \right)^{0.5} \left(\frac{e}{B} \right)^{1.2} \quad (5.11)$$

Using the Equation 5.11, R_{KR} has been calculated and compared with those calculated from experimental result as shown in Table 5.9.

Table 5.9 Comparison of predicted ultimate bearing capacity of reinforced sand bed with those
observed from experiment

B/L	N	d_f/B	e/B	$q_{u(Expt)}$	$q_{u(pred)}$	%Deviation
0.5	2	0.6	0.05	198	197	0.50
		0.6	0.1	165	166	-0.60
		0.6	0.15	132	133	-0.75
	3	0.85	0.05	238	236	0.84
		0.85	0.1	189	191	-1.05
		0.85	0.15	140	142	-1.42
	4	1.1	0.05	314	312	0.63
		1.1	0.1	237	244	-2.95
		1.1	0.15	164	169	-3.05
0.33	2	0.6	0.05	201	197	1.99
		0.6	0.1	171	166	2.92
		0.6	0.15	140	133	5.00
	3	0.85	0.05	242	236	2.47
		0.85	0.1	195	191	2.05
		0.85	0.15	151	142	5.96
	4	1.1	0.05	323	312	3.40
		1.1	0.1	251	244	2.78
		1.1	0.15	182	169	7.14

SUMMARIZED RESULTS AND SCOPE OF FUTURE WORK

A number of laboratory model tests have been conducted to determine the ultimate load bearing capacity of rectangular model footings resting over geogrid reinforced sand and subjected to vertical eccentric load. All the tests have been conducted for footing resting on the surface.

Following are the summarized results of present research work.

- The ultimate bearing capacity of the foundation for un-reinforced and reinforced soil decreases with the increase in eccentricity ratio i.e. e/B .
- The ultimate bearing capacity of the foundation increases with the increase in number of reinforcement layer.
- Reduction factor for the footing with $B/L=0.5$ & 0.33 has been derived separately and then combined to get a simple generalized equation of reduction factor for rectangular footing as shown in Equation 5.11.
- A comparison of the experiment and predicted ultimate bearing capacity for rectangular footings on reinforced sand bed by using concept of reduction factor is calculated using the derived relation and presented in Table 5.9. The maximum deviation of experimental from predicted is 7.14%.

SCOPE OF FUTURE WORK

The present research work is related to bearing capacity of eccentrically loaded rectangular footing with $B/L = 0.5$ & 0.33 resting over reinforced sand bed. Due to time constraint, other aspects related to shallow foundations could not be studied. The future work should consider the below mentioned points:

- The present work can be extended for footing with different B/L ratio and the result can be correlated with the result of present work.
- A generalized equation for ultimate bearing capacity of reinforced sand bed can be derived for any shape (i.e. square, rectangular and strip) of footing.

REFERENCES

1. Basudhar, P. K., Dixit, P. M., Gharpure, A., Deb, K. (2008). "Finite element analysis of geotextile-reinforced sand-bed subjected to strip loading." *Geotextiles and Geomembranes*, 26, pp. 91-99.
2. Behera, R. N. (2012). "Behaviour of shallow strip foundation on granular soil under eccentrically inclined load." *Ph.D Thesis*, NIT Rourkela.
3. Balla, A. (1962) "Bearing capacity of foundations." *J. Soil Mech. and Found. Div.*, ASCE, 88(5), pp. 13-34.
4. Bolt, A. (1982). "Bearing capacity of a homogeneous subsoil under rigid footing foundation loaded with inclined and eccentric force." *Inżynieria Morska*, 3(2), pp. 108-110.
5. Cichy, W., Dembicki, E., Odrobinski, W., Tejchman, A., and Zadroga, B. (1978). *Bearing capacity of subsoil under shallow foundations: study and model tests*. Scientific Books of Gdansk Technical University, Civil Engineering 22, pp. 1-214.
6. Dash, S. K., Krishnaswamy, N. R., Rajagopal, K. (2001). "Bearing capacity of strip footings supported on geocell-reinforced sand." *Geotextiles and Geomembranes*, 19, pp. 235-256.
7. Das, B. M., Omar, M. T. (1994). "The effect of foundation width on model tests for the bearing capacity of sand with geogrid reinforcement." *Geotechnical and Geological Engineering* 12, pp133-141.
8. Das, B. M., Shin, E. C., Omar, M. T. (1994). "The bearing capacity of surface strip foundations on geogrid-reinforced sand and clay – a comparative study." *Geotechnical and Geological Engineering* 12, pp1-14.

9. Das, B. M., "Shallow Foundation, Second Edition." *CRC Press*.
10. Das, B. M., "Principles of Foundation Engineering, Seventh Edition." *CENGAGE Learning*.
11. DeBeer, E. E. (1970), "Experimental determination of the shape factors of sand." *Geotechnique*. 20(4): 307.
12. Farah, C. A., "Ultimate Bearing Capacity of Shallow Foundations on Layered Soil." A *Thesis in the Department of Building, Civil and Environmental Engineering*, Concordia University, Canada.
13. GEOGRIDS, *Geosynthetics Specifier's Guide 2012*
14. Hansen, J. B. (1970). "A revised and extended formula for bearing capacity." Bulletin No. 28, *Danish Geotechnical Institute, Copenhagen*.
15. Hight W. H., Anders J. C. (1985) . "Dimensioning Footing Subjected to Eccentric Load." *Journal of Geotechnical Engineering* Vol 111, No.5.
16. Huang, C.C., and Menq, F.Y. (1997). "Deep-Footing and Wide-Slab effects in reinforced sandy ground." *Journal of Geotechnical and Geoenvironmental Engineering*, ASCE, 123(1), pp. 30-36.
17. Huang, C. C., Tatsuoka, F. (1990). "Bearing capacity of reinforced horizontal Sandy ground." *Geotextile and Geomembrane* 9, pp51-82.
18. Ingra, T.S., and Baecher, G.B. (1983). "Uncertainty in bearing capacity of sands." *J. Geotech. Eng.*, ASCE, 109(7), pp. 899-914.
19. Khing, K. H., Das, B. M., Puri, V. K., Cook, E. E., Yen, S. C. (1993). "The bearing capacity of strip foundation on geogrid reinforced sand." *Geotextile and Geomembrane* 12, pp351-361.

20. Kolay, P. K., Kumar, S., Tiwari, D. (2013). "Improvement of bearing capacity of shallow foundation on geogrid reinforced silty clay and sand." *Journal of Construction Engineering*.
21. Kumar A., Saran S. (2003). "Bearing Capacity of rectangular footing on reinforced soil." *Geotechnical and Geological Engineering* 21, pp201-224 .
22. Kumar A. ,Ohri M. L., Bansal R. K. (2013). "Pressure settlement charecteristics of strip footings on reinforced layered soil." *International Journal of Civil and Structural Engineering* Vol. 4, No. 2.
23. Kumar A. ,Ohri M. L., Bansal R. K. (2007). "Bearing capacity tests of strip footing on reinforced layer soil." *Geotechnical and Geological Engineering* 25, pp139-150.
24. Kumar, A., Walia, B. S., Saran, S. (2005). "Pressure-settlement charecteristics of rectangular footings on reinforced sand." *Geotechnical and Geological Engineering* 23, pp469-481.
25. Latha G.M., Somwanshi A. (2009). "Bearing Capacity of square footings on geosynthetic reinforced sand." *Geotextile and Geomembrane* 27, pp 281-294.
26. Meyerhof G.G. (1953). "An Investigation for the Foundations of a Bridge on Dense Sand." *Proceedings of the 3rd International Conference on Soil Mechanics and Foundation Engineering*, 2, pp. 66-70.
27. Meyerhof G. G. (1963). "Some recent research on the bearing capacity of foundation." *Canadian Geotech. J.* 1(1), pp 16.
28. Michalowski, R. L. (1997). "An estimate of the influence of soil weight on bearing capacity using limit analysis." *Soils and Foundations*. 37(4).

29. Milovic, D.M. (1965). "Comparison between the calculated and experimental values of the ultimate bearing capacity." *Proc., 6th ICSMFE, Montreal 1965*, 2, pp. 142-144.
30. Nareeman, B. J. (2012), "A study on the scale effect on bearing capacity and settlement of shallow foundation." *International Journal of Engineering and Technology Volumn 2 No. 3*.
31. Omar, M. T. (2006). "Ultimate bearing capacity of eccentrically loaded strip foundation on geogrid-reinforced sand." *Journal of Pure & Applied Sciences Volumn 3, No. 2*.
32. Patra, C.R., Das, B.M., Atalar, C. (2005). "Bearing capacity of embedded strip foundation on geogrid-reinforced sand." *Geotextiles and Geomembranes*, 23, pp. 454-462.
33. Patra, C.R., Das, B.M., Bhoi, M., Shin, E.C. (2006). "Eccentrically loaded strip foundation on geogrid-reinforced sand." *Geotextiles and Geomembranes*, 24, pp. 254-259
34. Peck, R. B., Hanson, W. E., Thornburn, T. H., "Foundation Engineering, Second Edition." *John Wiley & Sons*.
35. Prakash, S., Saran, S. (1971). "Bearing capacity of eccentrically loaded footings." *Journal of Soil Mechanics and Foundation*, ASCE, 97(1), pp. 95-118.
36. Purkayastha, R.D., Char, R.A.N. (1977). "Sensitivity analysis for eccentrically loaded footings." *J.Geotech.Eng. Div.*, ASCE, 103(6), 647.
37. Sadoglu E., Cure E., Moroglu B., Uzuner B.A. (2009). "Ultimate load for eccentrically loaded model shallow strip footings on geotextile-reinforced sand ." *Geotextiles and Geomembranes*, 27, pp. 176-182.
38. Sahu, R., Behera, R.N., Patra, C.R., (2013). "Bearing capacity prediction of eccentrically loaded footing on reinforced sand by ANN" *The 5th International Geotechnical Symposium-Incheon, 22-24 May, 2013*, pp.407-414.

39. Schlosser, F., Jacobsen, H. M., Juran, I. (1983). "Soil reinforcement—general report." *Proc. VIII European Conf. Soil Mech. Found. Engg.* Helsinki, Balkema.
40. Shin, E. C., Das, B. M., Lee, E. S., and Ataler, C., (2002). "Bearing capacity of strip foundation on geogrid-reinforced sand." *Geotechnical and Geological Engineering* 20: pp169-180.
41. Technical Engineering and Design Guides as Adapted from the US Army Corps of Engineers, No. 7." *American Society of Civil Engineers*".
42. Terzaghi, K. (1943). *Theoretical Soil Mechanics*, Wiley, New York.
43. Terzaghi, K., and Peck, R.B. (1948). *Soil mechanics in engineering practice*, 1st Edition, John Wiley & Sons, New York.
44. Vesic, A.S. (1973). "Analysis of ultimate loads of shallow foundations." *J. of Soil Mech. and Found. Div.*, ASCE, 99(1), pp. 45-73.
45. Yetimoglu T., Jonathan T. H. W., Saglamer A. (1994). "Bearing capacity of rectangular footings on geogrid-reinforced sand." *Journal of Geotechnical Engineering*, ASCE, 120, 12.
46. Zhao, A. (1996). "Failure Load on Geosynthetic Reinforced Soil Structure." *Geotextile and Geomembranes* 14, pp 289-300.

PUBLISHED PAPER

1. Shamshad Alam, Sunil Khuntia, Chittaranjan Patra (2014). “Prediction of compression index of clay using artificial neural network.” *International Conference on Industrial Engineering Science and Application – 2014*, (IESA-2014) , pp.387-390.